



Hydrogeochemistry Dataset obtained from Stygofauna Sampling, Pilbara Region, Western Australia

Data Release: Accompanying Notes

David J. Gray

EP162311

June 2016

Citation

Gray, David J. (2016). Hydrogeochemistry Dataset from Stygofauna Sampling, Pilbara Region, Western Australia: Data Release: Accompanying Notes. CSIRO, Australia. EP162311 32p

Copyright and disclaimer

© 2016 CSIRO. To the extent permitted by law, all rights are reserved and no part of this publication covered by copyright may be reproduced or copied in any form or by any means except with the written permission of CSIRO.

Important disclaimer

CSIRO advises that the information contained in this publication comprises general statements based on scientific research. The reader is advised and needs to be aware that such information may be incomplete or unable to be used in any specific situation. No reliance or actions must therefore be made on that information without seeking prior expert professional, scientific and technical advice. To the extent permitted by law, CSIRO (including its employees and consultants) excludes all liability to any person for any consequences, including but not limited to all losses, damages, costs, expenses and any other compensation, arising directly or indirectly from using this publication (in part or in whole) and any information or material contained in it.

Table of Contents

1	Introduction	1
2	The Stygo Pilbara Groundwater Dataset	1
2.1	Wells	1
2.2	Sampling.....	2
3	Data QA/QC Workflow	2
3.1	General Conversions	2
3.2	Filtering dataset for well contamination	2
3.3	Filtering dataset for surface water dilution	3
3.4	Alkalinity, pH and Eh	4
3.5	Salinity and Major Ions.....	5
3.6	Nitrogen and Phosphorus	7
3.7	Minors.....	7
4	Determination of “Contamination” Values and Factors	9
4.1	Contamination Criteria.....	9
4.2	Calculation of Contamination Values and Factor Classes	10
4.3	Data culling based on calculated Contamination	10
5	Element Indices	11
5.1	Ion Ratios	11
5.2	Ion Excess or Deficit	12
6	Solution Modelling	13
6.1	Activity Plots.....	13
6.2	Mineral Saturation Indices	14
7	Some Results	16
8	Conclusion	31
	References	32

Table of Figures

Figure 1: Stygofauna project groundwater samples, with CSIRO and Geological Surveys, Geoscience Australia Curnamona and Great Artesian Basin sampling, and State datasets.....	1
Figure 2: Stygo Pilbara groundwater samples, with CSIRO and Geological Surveys, and WA State samples. Purple squares represent the Stygofauna samples that were not included in the final corrected dataset.....	2
Figure 3: Initial HCO_3 vs. pH, and results following QA/QC correction of the Stygo Pilbara groundwater dataset.....	4
Figure 4: Initial Eh vs. pH, and results following QA/QC correction of the Stygo Pilbara dataset	5
Figure 5: Initial Balance vs. TDS, and results following QA/QC correction of the Stygo Pilbara groundwater dataset.....	6
Figure 6: Initial K vs. Na, and results following QA/QC correction of the Stygo Pilbara groundwater dataset.....	6
Figure 7: Initial Mg vs. Na, and results following QA/QC correction of the Stygo Pilbara groundwater dataset.....	6
Figure 8: Initial Sr vs. Ca, and results following QA/QC correction of the Stygo Pilbara groundwater dataset.....	7
Figure 9: Initial SO_4 vs. Cl, and results following QA/QC correction of the Stygo Pilbara groundwater dataset.....	7
Figure 10: Initial Total N vs. pH, and results following QA/QC correction of the Stygo Pilbara groundwater dataset.....	8
Figure 11: Initial P vs. pH, and results following QA/QC correction of the Stygo Pilbara groundwater dataset.....	8
Figure 12: Initial Si vs. pH, and results following QA/QC correction of the Stygo Pilbara groundwater dataset.....	8
Figure 13: Initial Fe vs. pH, and results following QA/QC correction of the Stygo Pilbara groundwater dataset.....	9
Figure 14: Initial Mn vs. pH, and results following QA/QC correction of the Stygo Pilbara groundwater dataset.....	9
Figure 15: Dissolved Ca vs. Na for the corrected Stygo Pilbara groundwater dataset, coloured by the CaNaSW range.....	12
Figure 16: Dissolved Ca vs. Na for the corrected Stygo Pilbara groundwater dataset, coloured by the CaNaDSW range.	13
Figure 17: Modelled Eh-pH plot of Fe speciation overlain with Eh:pH data for the corrected Stygo Pilbara groundwaters.	14
Figure 18: Modelled Eh-pH plot of Fe speciation (crystalline Fe oxides not involved) overlain with Eh:pH data for the corrected Stygo Pilbara groundwaters.	14
Figure 19: Gypsum Saturation Index (SI) vs. TDS for the corrected Stygo Pilbara groundwater dataset, grouped by the defined saturation level.....	15
Figure 20: Calcite Saturation Index (SI) vs. pH for the corrected Stygo Pilbara groundwater dataset, grouped by the defined saturation level.....	15
Figure 21: TDS distribution across Australia and in the Pilbara Craton.	17
Figure 22: Groundwater pH distribution across Australia and in the Pilbara Craton.....	18

Figure 23: Groundwater Mg:Na Ion Ratio (MgNaSW) distribution across Australia and in the Pilbara Craton.....	19
Figure 24: Groundwater Ca:Na Ion Ratio (CgNaSW) distribution across Australia and in the Pilbara Craton.....	20
Figure 25: Groundwater Ca:Na Ion Difference (CaNaDSW) distribution across Australia and in the Pilbara Craton.....	21
Figure 26: Groundwater K:Na Ion Ratio (KNaSW) distribution across Australia and in the Pilbara Craton.....	22
Figure 27: Groundwater K:Na Ion Difference (KaNaDSW) distribution across Australia and in the Pilbara Craton.....	23
Figure 28: Groundwater Sr:Ca Ion Ratio (SrCaSW) distribution across Australia and in the Pilbara Craton.....	24
Figure 29: Groundwater SO ₄ :Cl Ion Ratio (SO ₄ ClSW) distribution across Australia and in the Pilbara Craton.....	25
Figure 30: Groundwater gypsum saturation distribution across Australia and in the Pilbara Craton.....	26
Figure 31: Groundwater celestine saturation distribution across Australia and in the Pilbara Craton.	27
Figure 32: Groundwater silica saturation distribution across Australia and in the Pilbara Craton.	28
Figure 33: Groundwater NO ₃ concentration distribution across Australia and in the Pilbara Craton.....	29
Figure 34: Groundwater Calcite saturation distribution across Australia and in the Pilbara Craton.	30

1 Introduction

This is the accompanying notes to the revised hydrogeochemical dataset from the Stygofauna sampling of the Pilbara region, Western Australia (WA) (Halse et al., 2014), courtesy of Mike Scanlon, Bennelongia Environmental Consultants. This revised dataset is available online (Gray, 2016a; <http://doi.org/10.4225/08/575CDF639A59A>), and users can also contact the author. By combining data into one file, with consistent detection limits, correcting for analytical differences, and comparing with recent data, these data should now be readily usable and “seamlessly” comparable. This data release is part of the “Continental Scale Hydrogeochemistry” initiative (Figure 1).

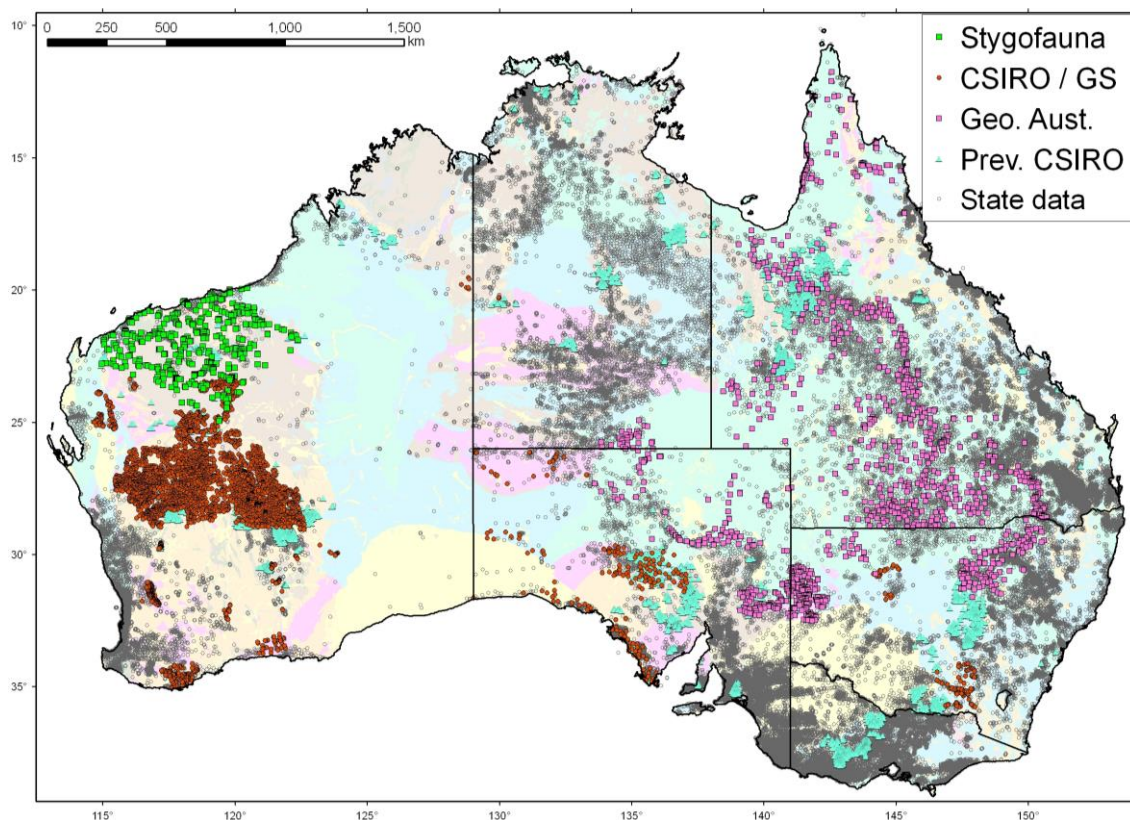


Figure 1: Stygofauna project (Halse et al., 2014) groundwater samples (green squares), with CSIRO and Geological Surveys (Forbes et al., 2013; Giblin, 2001; Gray, 2016b; Gray et al. 2012, 2015, 2016), Geoscience Australia Curnamona (de Caritat et al. 2005) and Great Artesian Basin (Radke et al., 2000) sampling, and State datasets (Bardwell and Gray, 2016a,b,c; Gray and Bardwell, 2016a,b,c).

2 The Stygo Pilbara Groundwater Dataset

This dataset is hereafter described as the Stygo Pilbara dataset. Sampling and analysis information is summarised from Halse et al. (2014).

2.1 Wells

The sampling program was conducted from 2002 to 2005, within and directly south of the Pilbara Craton, WA (Figure 2), with 1053 samples collected from 507 wells and drill holes. Larger (up to 2 m diameter) wells were mostly older, with shallower water-tables and rock-lined. Narrower wells were cased (PVC or steel) and slotted below the water table. Details of slotting and screens were usually not available. All wells sampled were more than 6 months old, and most were capped.

Electrical Conductivity (EC), pH, Eh, and dissolved oxygen (DO) were measured using a Yeo-Kal 611 water quality analyser at 1 m below the watertable. Depths to water, and the base of the well were measured with a Richter Electronic Depth Gauge or weighted Lufkin tape measure.

2.2 Sampling

Water was collected from 1 m below the watertable using a sterile bailer (Clearwater PVC disposable 38 x 914 mm) and a 250 mL sample was collected for analysis of total dissolved solids (TDS), solute composition (Na, K, Mg, Ca, Sr, Cl, SO₄, Si, Fe, Mn), alkalinity, colour and turbidity. A second 125 mL sample was frozen in the field for later analysis for total soluble N, nitrate/nitrite, total soluble P and soluble reactive P by ChemCentre, Perth using standard methods (APHA, 1995).

3 Data QA/QC Workflow

3.1 General Conversions

The object of this study was to produce a single, robust groundwater dataset from the Stygo Pilbara dataset that could be combined with other datasets across Australia. All the groundwater data and logging provided were combined. For ease of analysis and plotting, all "<" were changed to "-", and all sample lines with no chemical data were removed. Data were examined and where problems were apparent, values, or indeed data lines were deleted. Such deletions represent a minor proportion (Figure 2) of the samples.

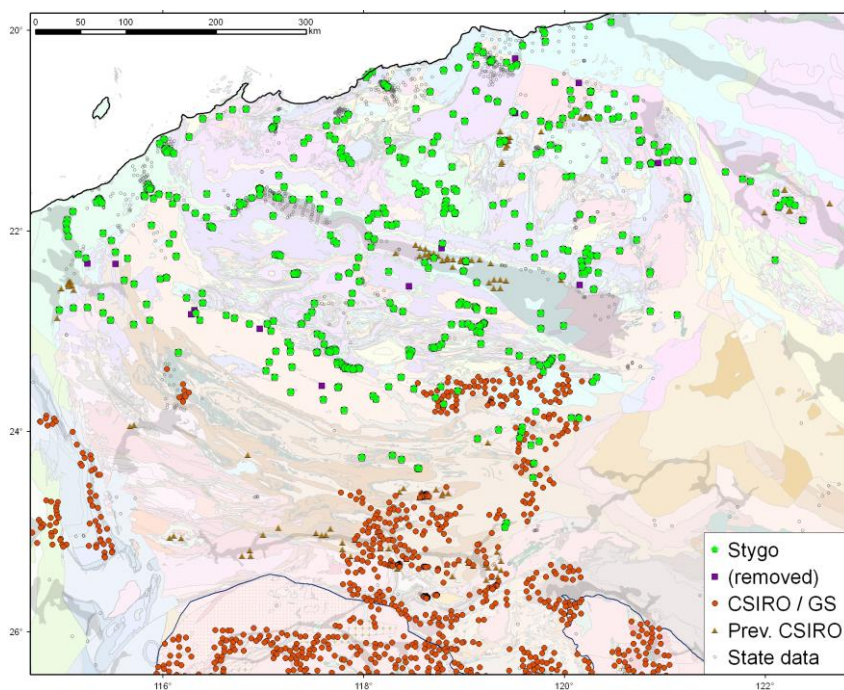


Figure 2: Stygo Pilbara (Halse et al., 2014) groundwater samples (green), with CSIRO and Geological Surveys (Giblin, 2001; Gray, 2016b; Gray et al. 2016), and WA State (Bardwell and Gray, 2016c) samples. Purple squares represent the Stygofauna samples that were not included in the final corrected dataset.

3.2 Filtering dataset for well contamination

Some of the groundwater samples had various forms of contamination, such as dead animals, and other biological and anthropogenic (e.g. hydrocarbons) contaminants. Field logs were examined and samples with "animal in bore", "oily" or "smell" checked. As discussed later (Section 4.1), various metrics can be higher in contaminated waters, particularly Colour, P, NH₃ (calculated as total N minus NO₃_N) and, to a lesser degree Fe and Mn. These were all checked. Potentially contaminated samples were examined and checked against duplicate or adjacent samples. The following samples were removed from the dataset:

- *G70830105P* - extreme Fe, Mn, low Si.
- *ROY002* - extreme NH₃, P, Colour, animal in bore.
- *126/3* - extreme NH₃, P, Colour, high Fe, Mn. Frogs in bore. Machine oil (or organic) smell, sample bottle lathered
- *WW8-4 2/10/2005* - High colour
- *NWCHSLK864* - extreme NH₃, P, High Colour
- *GNHSLK1380* - extreme NH₃, P, High Colour
- *MS-2C 20/11/2003* - Moderate Fe, has less data and moderately differs from Dup
- *MIN003* - extreme NH₃, high Fe, Mn. Animal in well
- *YROB5* - extreme NH₃, P, high Fe, Mn. Reduced, differs from adjacent bore
- *MILLPAN#1 25/06/2004* - extreme NH₃, P, high Fe, Mn. Reduced, differs from adjacent bore
- *DGE3* - extreme NH₃, P, high Fe, Mn. Dead reptile in bore
- *NWSLK176* - extreme NH₃, high Fe, Mn.
- *HEOP0462 10/04/2003* - extreme NH₃, high P, Fe, Mn. Differed from Dup
- *WYL001* - high NH₃, low SO₄. Well in poor condition
- *WYL003* - high NH₃. Differed from Adjacent bores
- *ASH008 16/08/2004* - high NH₃, low SO₄. Differed from Dup
- *WAR16* - high NH₃, Oily residue, differed from adjacent bores
- *SG1* - high NH₃, Animal in Bore
- *GNHSLK1648B 16/11/2002 - 12/05/2004* - high NH₃, mod Fe, Mn. Differed from Dups
- *PTO1-B* - high NH₃, mod Fe, Mn. Oily residue, differed from adjacent bores
- *PTO6* - high NH₃, mod Fe, Mn, low Si, SO₄. Differed from adjacent bores
- *PANNASLK24 1/08/2006* - high NH₃, mod fe, Mn, low Si, SO₄.
- *CR8/97* - high Fe, Mn, low Si, SO₄. Differed from other bores in Bore Field
- *MINI004* - high NH₃, low SO₄, Si. Animal in Bore
- *NWSLK324C* - high NH₃. Differed from Adj
- *NA1M2 & NA1M5 7/04/2003* - high NH₃, P. Differed from Dups
- *W275 & W276 10/04/2003* - high NH₃, P, Fe, Mn. Differed from Dups
- *MBSLK352* - high NH₃, P, Fe, Mn. Differed from Dups
- *NWCHSLK822 26/06/2004* - high NH₃, P, Fe, Mn. Differed from Dup
- *HILLSIDE 5 18/07/2004* - high NH₃, P, Fe, Mn. Differed from Dup
- *ONSLOWSLK20 23/07/2004* - high NH₃, P, Fe, Mn. Differed from Dup
- *MEEN3 6/05/2005* - high NH₃, P, Mn. Differed from Dup
- *OnslowSLK8 6/08/2005* - high NH₃, P, Mn. Dead stuff and maggots. Differed from Dup
- *WAWB54 14/10/2004* - high Colour, P, Mn. Differed from Dup
- *ASH006 5/06/2005* - high NH₃, P, Mn. Differed from Dup
- *NWSLK136 20/10/2004* - extreme NH₃, P, high Fe, Mn. Bore in poor condition
- *DGE2A 12/06/2003* - high Fe, Mn.
- *PSPRLK48 26/07/2003* - high Mn, low Si. Differed from Dup's
- *MBSLK400A 13/06/2003 & 13/05/2004* - high P
- *MBSLK356B 4/10/2005* - high NH₃
- *PFO5-3 28/09/2005 & 20/05/2004* high NH₃, post cyclone
- *PANNASLK12 1/08/2003* - high N, low Si. Rotten animal smell in bore.
- *GNHSLK1631* - high NH₃, P. Bore is commonly dry
- *YM0109 25/11/2002* - high NO₃, P
- *MBSLK344 13/05/2004 & 4/10/2005* - high NH₃, P, Mn. Differed from other dup's.

3.3 Filtering dataset for surface water dilution

For un-capped wells, there is the potential for surface water ingress, diluting the “true” groundwater chemistry, as well as possibly adding contamination. This would have been a particular issue immediately after the major cyclone events of March, 2004. Logs, sample dates and evidence for dilution (e.g. lower salinity than other duplicates) were checked and the following samples removed from the dataset:

- *WYL004 12/08/2004* - Fresher than Dup
- *GNHSLK1804 5/08/2005* - high N, low Si. Fresher than Dup
- *NWSLK344 18/05/2004* - Much Fresher than Dup
- *PTO2 17/10/2004* - Fresher than Dup
- *MS-8B 22/10/2004* - Fresher than Dup

- HB445 15/05/2004 - Much Fresher than Dup
- HB449 15/05/2004 - Much Fresher than Dup
- HB240 15/05/2004 - Fresher than Dup
- HB406 16/05/2004 - Fresher than Dup

3.4 Alkalinity, pH and Eh

Alkalinity was measured in varying ways: e.g., as HCO_3^- , CO_3^{2-} and CaCO_3 equivalencies. All data was recalculated as HCO_3^- equivalency and combined. Alkalinity data for dissolved Fe > 5 mg/L were removed as acid production during oxidation after sampling can reduce alkalinity. All low pH (< 6) samples were checked. Where they had erroneously high alkalinity and/or duplicates with much higher pH, the pH values were deleted (Figure 3). Based on discussion of field methodology pH error is estimated to be > 0.5 units.

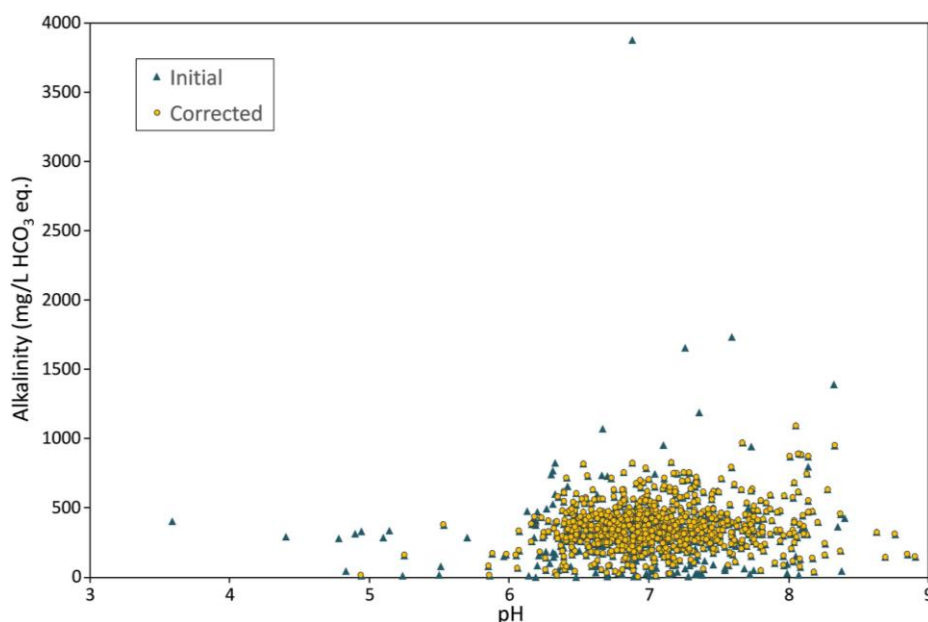


Figure 3: Initial HCO_3^- vs. pH, and results following QA/QC correction of the Stygo Pilbara groundwater dataset.

The redox data (as Eh in mV, relative to the standard hydrogen electrode) is commonly plotted against pH (Figure 4) as an aid to understanding the redox condition of the environment. The winnowing of contaminated samples (see above) has strongly reduced the number of low Eh samples (Figure 4). This is expected, as samples contaminated with organic matter, oil and/or dead animals will have erroneously low Eh. Of particular note are the pH and Eh values for the June '03 sampling, with all pH values less than 6.5 and all but 2 Eh values above 500 mV (Figure 4). These values generally differ strongly from sample duplicates for other dates and appear to be instrumental artefacts or errors of some kind. Other sampling and chemical parameters have good agreement with the sample duplicates, so it appears that only pH and Eh are in error for this period. Therefore, pH and Eh values (only) were deleted for this sample batch. Additionally, Eh measurements did appear to show instrumental drift over time, of the order of 100 - 200 mV, which was not corrected for. This potential should be taken into account when using Eh for interpretation and/or geochemical modelling.

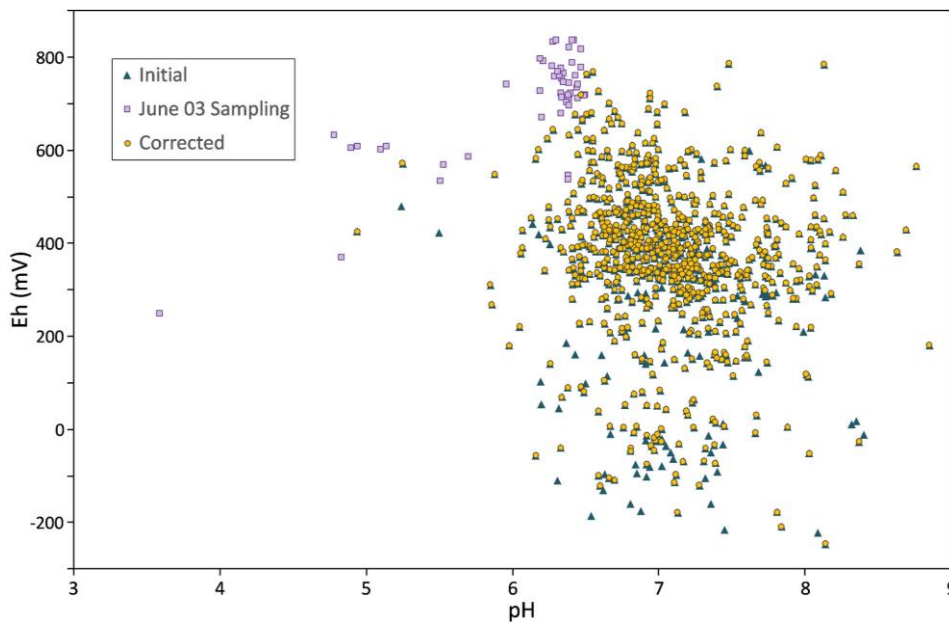


Figure 4: Initial Eh vs. pH, and results following QA/QC correction of the Stygo Pilbara dataset. Purple squares are pH/Eh data for June '03.

3.5 Salinity and Major Ions

Sulfate (SO_4) is assumed to be the dominant form of S in solution, which is likely for waters that are not highly reduced or organic-rich. Salinity (TDS as mg/L) was determined as the sum of all major ions, i.e.:

$$TDS = Na + K + Mg + Ca + Cl + SO_4 + 0.49 * HCO_3$$

This calculated TDS agreed closely with the TDS in the dataset.

Charge balance was calculated, according to:

$$\frac{(Na/22.99 + K/39.1 + Mg/12.15 + Ca/20.04) - (Cl/35.45 + SO_4/48.03 + HCO_3/61.02)}{(Na/22.99 + K/39.1 + Mg/12.15 + Ca/20.04) + (Cl/35.45 + SO_4/48.03 + HCO_3/61.02)}$$

This calculated balance was plotted against TDS (Figure 5). The electrical balance is expected to be zero, and the calculated balance should be between -0.05 and 0.05, except for very fresh waters for which other phases not used in the calculation can affect the calculated balance. All anomalous points were checked in the dataset. Where erroneous balance could be readily explained by a transposition error (e.g. Na concentration 10x too high due to decimal point being typed into the dataset incorrectly), the specific value was removed. Where the reason for erroneous balance could not be readily revealed as a transcription error, the data line was deleted. Many of these were the presumably contaminated (Section 0) or diluted (Section 3.3) groundwaters, with additional samples deleted being:

- CR10/97 2/08/2003 - Balance 0.16, Differed from Dup
- GNHSLK1066 10/08/2005 - Balance 0.14
- MILLYARRA64A 12/04/2003 - Balance 0.13
- WAR02 3/10/2005 - Balance 0.11

The various salinity effected ions were plotted: K (Figure 6), Mg (Figure 7) and Ca vs Na; Sr vs Ca (Figure 8); SO_4 vs Cl (Figure 9), so as to further check for any potentially erroneous data. Following on from the previous deletions, samples *Noreena01 15/07/2004* (Mg and Ca possibly 10x too low) and *HWE5 2/10/05* (Sr possibly 10x too low) were also deleted.

All the deletions listed above reduced the number of data lines from 1053 to 965, and the number of sample sites with chemical data from 486 to 466.

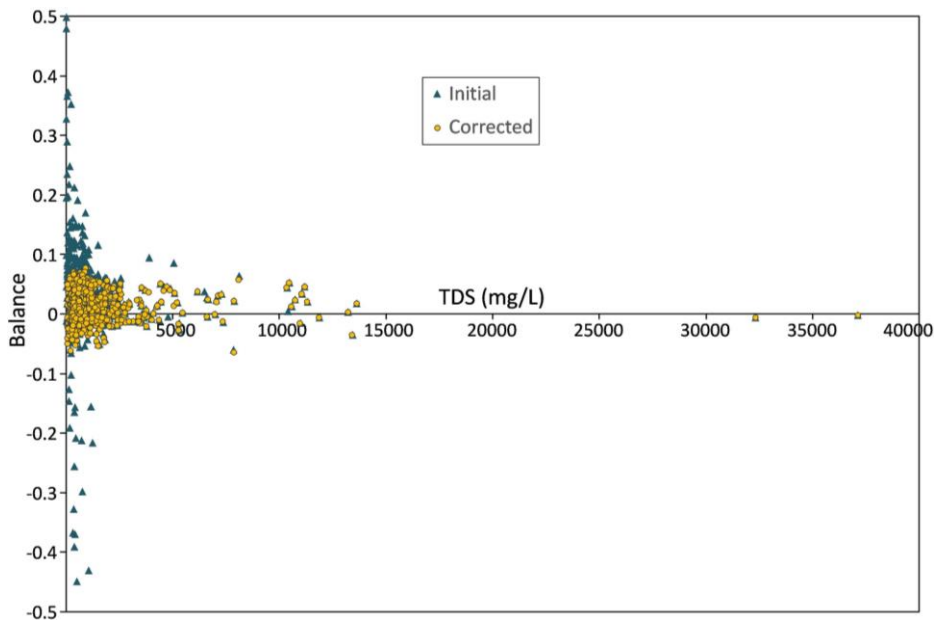


Figure 5: Initial Balance vs. TDS, and results following QA/QC correction of the Stygo Pilbara groundwater dataset.

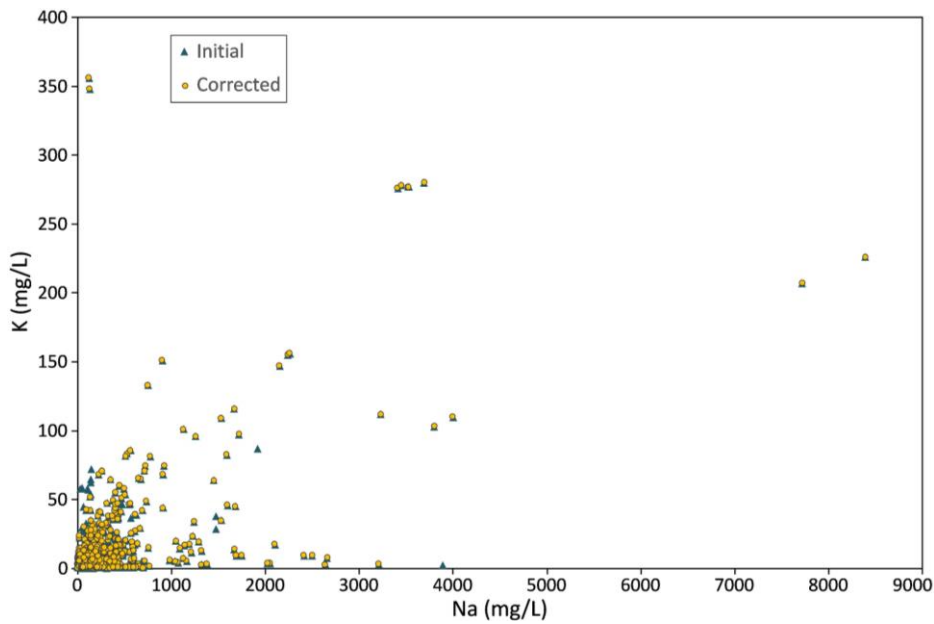


Figure 6: Initial K vs. Na, and results following QA/QC correction of the Stygo Pilbara groundwater dataset.

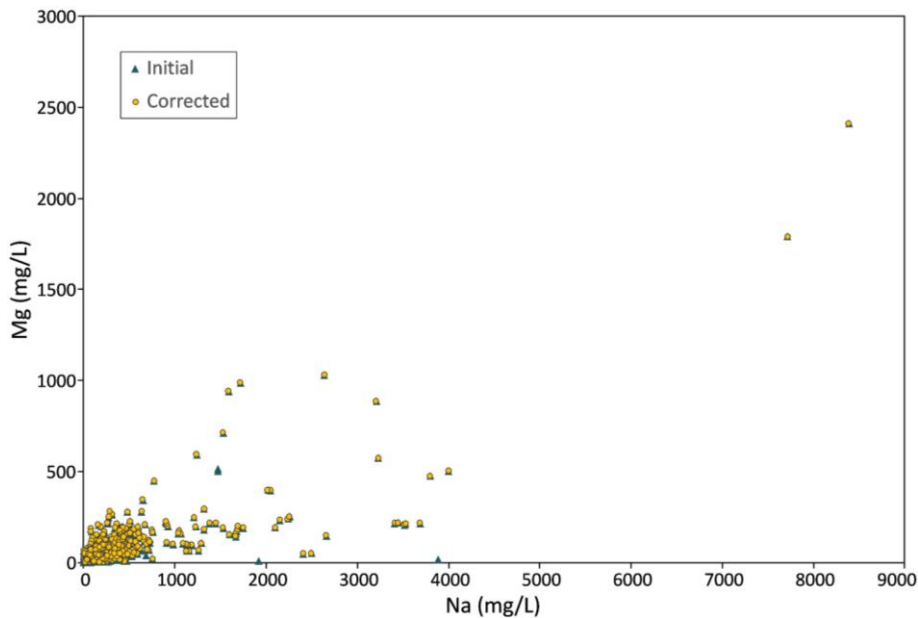


Figure 7: Initial Mg vs. Na, and results following QA/QC correction of the Stygo Pilbara groundwater dataset.

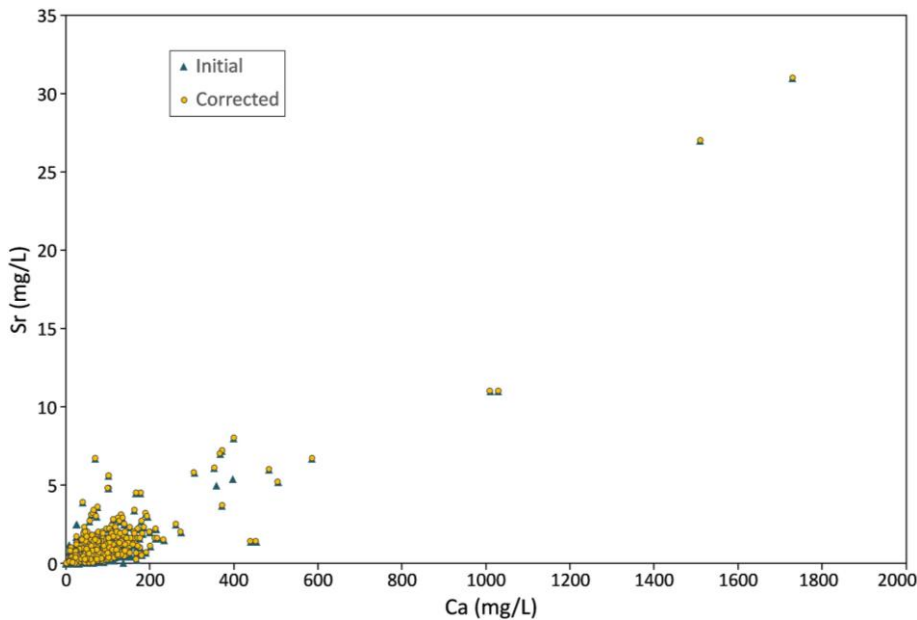


Figure 8: Initial Sr vs. Ca, and results following QA/QC correction of the Stygo Pilbara groundwater dataset.

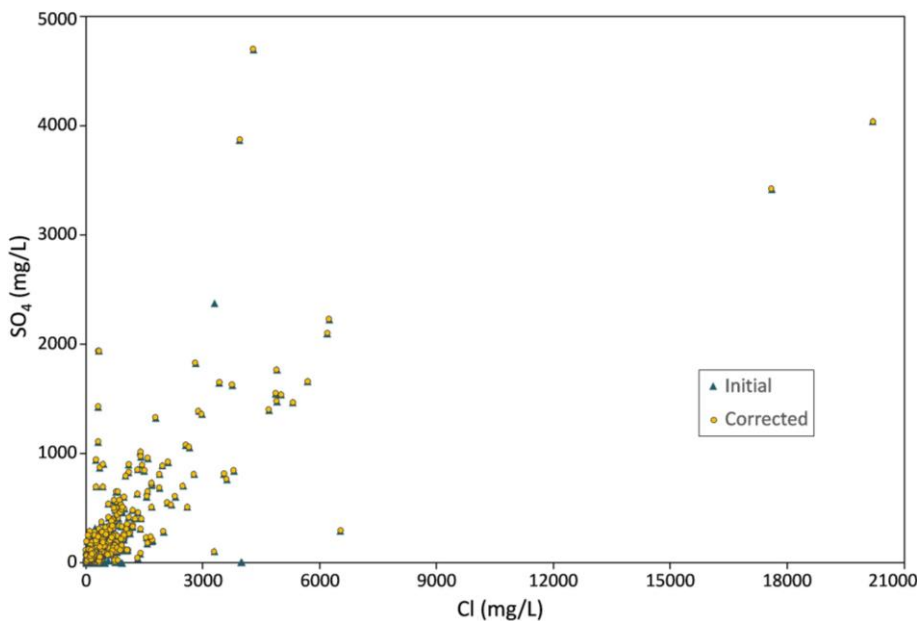


Figure 9: Initial SO₄ vs. Cl, and results following QA/QC correction of the Stygo Pilbara groundwater dataset.

3.6 Nitrogen and Phosphorus

Nitrogen data was commonly as NO₃_N and as total N, with NH₃_N sometimes analysed and closely approximated by [Total_N] – [NO₃_N]. For continuity, [NH₃_N] was calculated for all samples as [Total_N] - [NO₃_N]. The sample deletions described above (Sections 0 - 3.5) particularly effected high N samples (Figure 10), as these are commonly due to contamination. Similarly, many high P samples (P also tends to be high in contaminated waters) were winnowed (Figure 11) by the sample deletions.

3.7 Minors

For SiO₂, the 3 sample values greater than 150 mg/L were removed: such concentrations are above amorphous silica solubility, and are likely to be erroneous. Where SiO₂ values were less than 10 mg/L and the sample duplicate was greater than 5x this value, the low Si result is likely be due to Si depletion from dilution or contamination, and was deleted. For consistency with other data columns, SiO₂ was recalculated as Si equivalent, by dividing by 1.998 (Figure 12). The high Fe (Figure 13) and Mn (Figure 14) values in the original dataset were removed by the initial sample winnowing (Sections 0, 3.3 and 3.5).

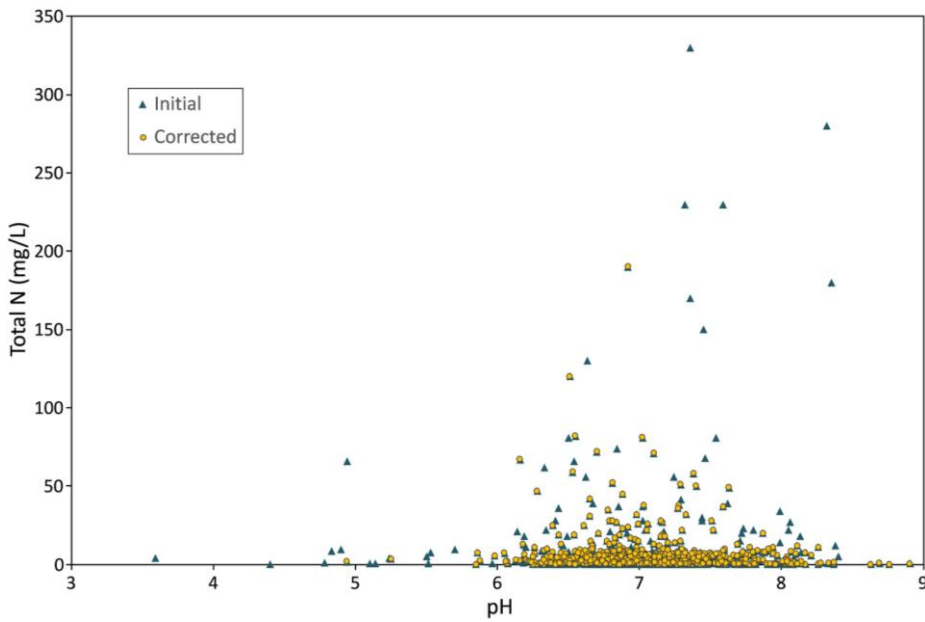


Figure 10: Initial Total N vs. pH, and results following QA/QC correction of the Stygo Pilbara groundwater dataset.

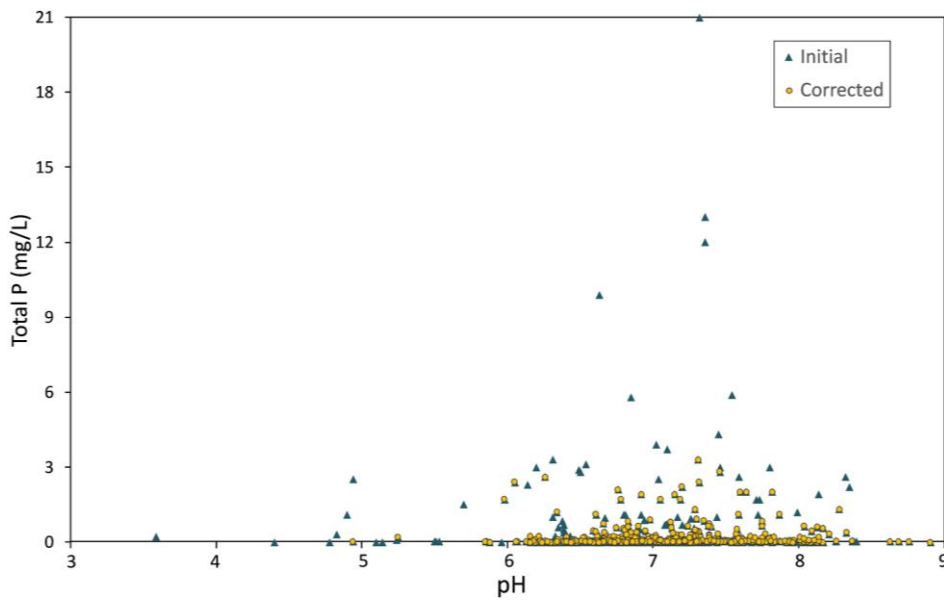


Figure 11: Initial P vs. pH, and results following QA/QC correction of the Stygo Pilbara groundwater dataset.

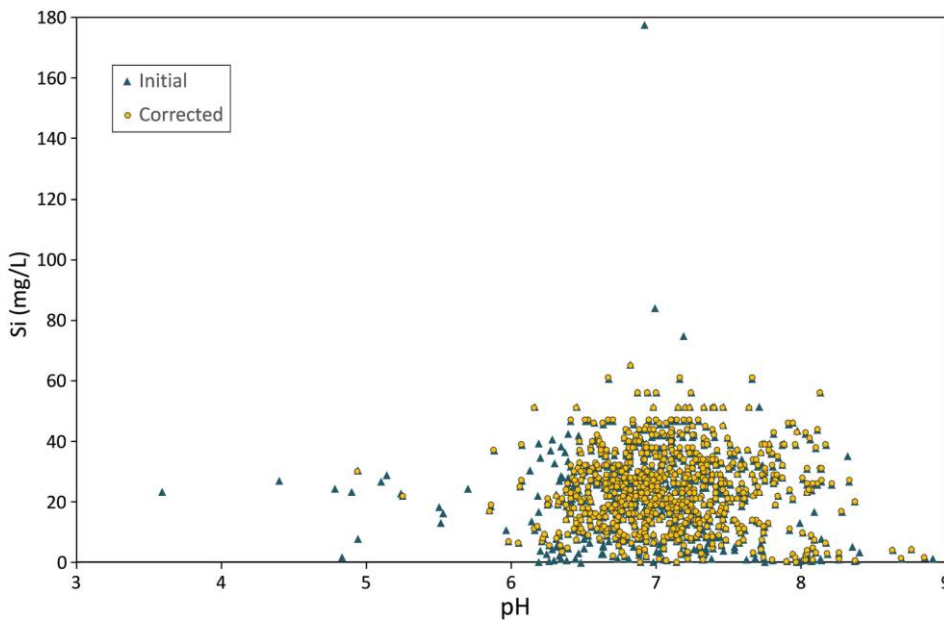


Figure 12: Initial Si vs. pH, and results following QA/QC correction of the Stygo Pilbara groundwater dataset.

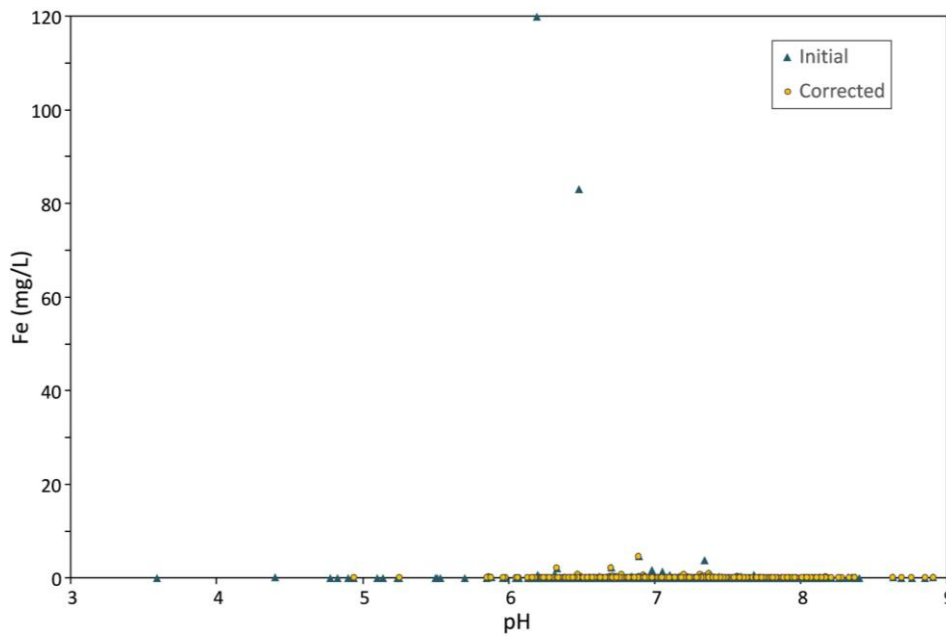


Figure 13: Initial Fe vs. pH, and results following QA/QC correction of the Stygo Pilbara groundwater dataset.

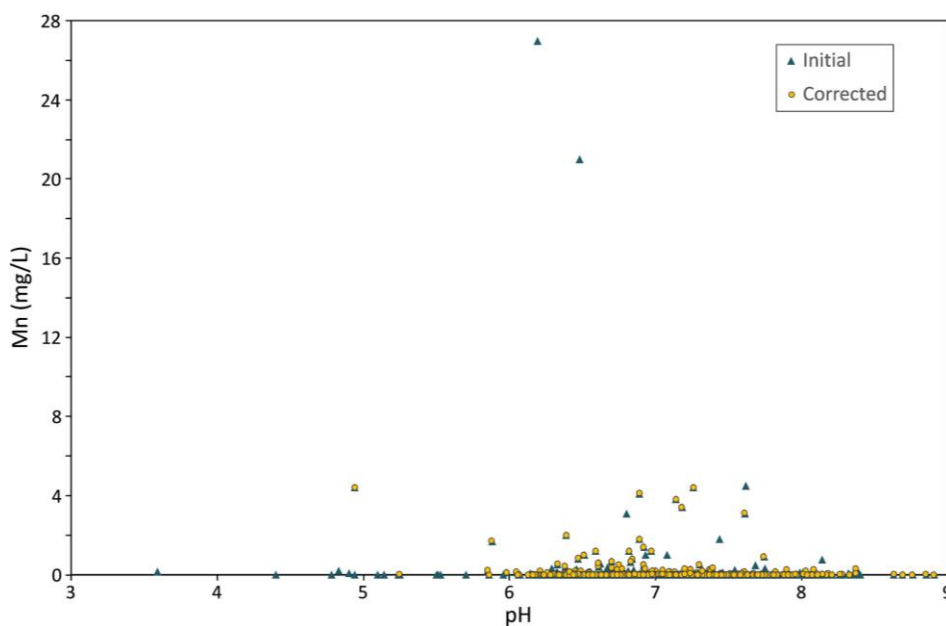


Figure 14: Initial Mn vs. pH, and results following QA/QC correction of the Stygo Pilbara groundwater dataset.

4 Determination of “Contamination” Values and Factors

4.1 Contamination Criteria

Although many of the most contaminated samples were already removed from the dataset, it is feasible that some weakly to moderately contaminated samples are still included. Previous research (Gray et al., 2016) has indicated methods to measure such contamination and quantify its effects on measured solute concentrations. Gray et al. (2016) indicated that, in central WA groundwaters, contaminated samples (as based on the state of the well and/or the colour and smell of the samples) had a number of clear differences:

- Significantly higher in at least one of dissolved organic carbon (DOC) and P (expected to be from biological sources), Mn (possibly reductive leaching), Fe and Zn (possibly from various sources including metallic materials);
- Significantly lower in various elements expected to be sensitive to reduction, such as SO_4 (when plotted relative to Cl) and NO_3 .

Other parameters also showed variation, such as Eh which was commonly lower in contaminated samples, and bicarbonate which trended towards higher values in contaminated samples (and weakly correlated with DOC). However, these two parameters were not useful in robustly determining contamination, as the contamination effects were less than the background variation.

4.2 Calculation of Contamination Values and Factor Classes

Gray et al. (2016) used DOC, PO₄, Mn, Fe and Zn to develop a contamination metric. Of these, P, Mn and Fe data are available for the Stygo Pilbara dataset. Therefore (based on Gray et al., 2016a), a “contamination value” (CV) was calculated for this dataset using:

$$CV = \text{Mean} \left(\log_{10} \frac{P}{0.277}, \log_{10} \frac{Fe}{0.234}, \log_{10} \frac{Mn}{0.059} \right)$$

(all elements in mg/L).

As in Gray et al., (2016), this CV value is used to split the samples in the dataset into 6 “contamination factor” (CF) classes (% shown is the proportion of each CF class of the entire dataset):

CF 1:	Flowing or purged bores	(other samples are bailed)	1.7%
CF 1.8:	CV < -0.8	(bailed, uncontaminated)	84.6%
CF 2.2:	-0.8 < CV < -0.417	(bailed, very slightly contaminated)	7.2%
CF3:	-0.417 < CV < -0.1	(bailed, slightly contaminated)	4.6%
CF4:	-0.1 < CV < 0.3	(bailed, contaminated)	1.6%
CF5:	0.3 < CV	(bailed, highly contaminated)	0.4%

Thus, over 86% of the final revised dataset are defined as uncontaminated, and including very slightly contaminated samples brings this up to 93.5% of all samples.

4.3 Data culling based on calculated Contamination

Based on analysis by Gray et al. (2016), the elemental data is culled, as listed in Table 1. Thus, for example, Eh, HCO₃, Mn, N, P and SO₄ are very sensitive to contamination, so data only for CF groups 1 and 1.8 are used (still 86.3% of the samples in the revised dataset), as opposed to TDS, for which data from CF groups 1 – 4 (99.4% of the samples) are used. This approach has been demonstrated to be successful for bailed samples using internal statistical analysis (Gray et al., 2016) and dataset comparisons (Gray, 2016b).

Table 1. Influence of contamination on each measured component for the Stygo Pilbara groundwater dataset: those with only CF Class 1.8 kept are the most influenced by contamination; whereas up to CF Class 4 kept indicates 99.6% of the whole data set was used.

Element	CF Kept	Element	CF Kept	Element	CF Kept
Eh	1.8	Total P	1.8	Mg	2.2
HCO ₃	1.8	Si	1.8	K	3
Mn	1.8	SO ₄	1.8	Sr	3
NH ₃	1.8	Fe	2.2	Na	4
NO ₃	1.8	pH	2.2	Cl	4
Total N	1.8	Ca	2.2	TDS	4

5 Element Indices

5.1 Ion Ratios

Using element ratios (compared to Cl or Na), some samples were observed to be in excess or deficit relative to the ion ratio observed for sea water. The distance away from the sea water dilution/evaporation trend line was determined, and provided a numerical measurement of the excess or depletion. This was done for; K, Mg, and Ca (Figure 15) with respect to Na, Mg and Sr with respect to Ca, and SO₄ with respect to Cl. At close scales (Gray and Noble, 2006), sulfate excess was particularly important for evaluating changes related to weathering sulfide ore bodies in shallow groundwater. At broader sampling (> km spacing), sulfate excess is more related to faults and other geological structures (Gray et al., 2016).

The other major element indices are strongly controlled by lithology and hydrothermal alteration. For example, Sr relative to Ca is useful in distinguishing basic and acid lithologies (Gray et al., 2016). The derived formulas are listed below. Note that the ratio used in each equation is the relevant ratio between the two elements in sea water. Two different equations are used for each ratio calculation; the variant for lower salinity (e.g., Na < 500 mg/L for KNaSW etc.) is derived so as to minimise issue for errors at low value of the denominator). Figure 15 provides a visible example of the variation in the relevant ratio.

$$\begin{aligned} \mathbf{KNaSW} &= [2 \times (\text{K} - 0.0363 \times \text{Na})] / [0.0363 \times (\text{Na} + 500)] && \dots \text{Na} < 500 \text{ mg/L} \\ &= [\text{K} - 0.0363 \times \text{Na}] / [0.0363 \times \text{Na}] && \dots \text{Na} \geq 500 \text{ mg/L} \end{aligned}$$

$$\begin{aligned} \mathbf{MgNaSW} &= [2 \times (\text{Mg} - 0.1194 \times \text{Na})] / [0.1194 \times (\text{Na} + 500)] && \dots \text{Na} < 500 \text{ mg/L} \\ &= [\text{Mg} - 0.1194 \times \text{Na}] / [0.1194 \times \text{Na}] && \dots \text{Na} \geq 500 \text{ mg/L} \end{aligned}$$

$$\begin{aligned} \mathbf{CaNaSW} &= [2 \times (\text{Ca} - 0.0381 \times \text{Na})] / [0.0381 \times (\text{Na} + 500)] && \dots \text{Na} < 500 \text{ mg/L} \\ &= [\text{Ca} - 0.0381 \times \text{Na}] / [0.0381 \times \text{Na}] && \dots \text{Na} \geq 500 \text{ mg/L} \end{aligned}$$

$$\begin{aligned} \mathbf{MgCaSW} &= [2 \times (\text{Mg} - 3.14 \times \text{Ca})] / [3.14 \times (\text{Ca} + 20)] && \dots \text{Ca} < 20 \text{ mg/L} \\ &= [\text{Mg} - 3.14 \times \text{Ca}] / [3.14 \times \text{Ca}] && \dots \text{Ca} \geq 20 \text{ mg/L} \end{aligned}$$

$$\begin{aligned} \mathbf{SrCaSW} &= [2 \times (\text{Sr} - 0.0195 \times \text{Ca})] / [0.0195 \times (\text{Ca} + 20)] && \dots \text{Ca} < 20 \text{ mg/L} \\ &= [\text{Sr} - 0.0195 \times \text{Ca}] / [0.0195 \times \text{Ca}] && \dots \text{Ca} \geq 20 \text{ mg/L} \end{aligned}$$

$$\begin{aligned} \mathbf{SO_4ClSW} &= [2 \times (\text{SO}_4 - 0.1396 \times \text{Cl})] / [0.1396 \times (\text{Cl} + 500)] && \dots \text{Cl} < 500 \text{ mg/L} \\ &= [\text{SO}_4 - 0.1396 \times \text{Cl}] / [0.1396 \times \text{Cl}] && \dots \text{Cl} \geq 500 \text{ mg/L} \end{aligned}$$

The different calculation methods for lower ion concentrations are to minimise skewing data due to analytical errors close to detection limits. At higher concentrations these become a ratio difference:

e.g. for Na > 500 mg/L

- CaNaSW = 12 means the Ca/Na sample ratio is 13 x sea water
- CaNaSW = 6 means the Ca/Na sample ratio is 7 x sea water
- CaNaSW = 2.5 means the Ca/Na sample ratio is 3.5 x sea water
- CaNaSW = 1 means the Ca/Na sample ratio is 2 x sea water
- CaNaSW = 0.3 means the Ca/Na sample ratio is 1.3 x sea water
- CaNaSW = 0 means the Ca/Na sample ratio is at the sea water value
- CaNaSW = -0.1 means the Ca/Na sample ratio is 0.9 x sea water
- CaNaSW = -0.4 means the Ca/Na sample ratio is 0.6 x sea water
- CaNaSW = -0.8 means the Ca/Na sample ratio is 0.2 x sea water

This is demonstrated for Ca:Na in Figure 15.

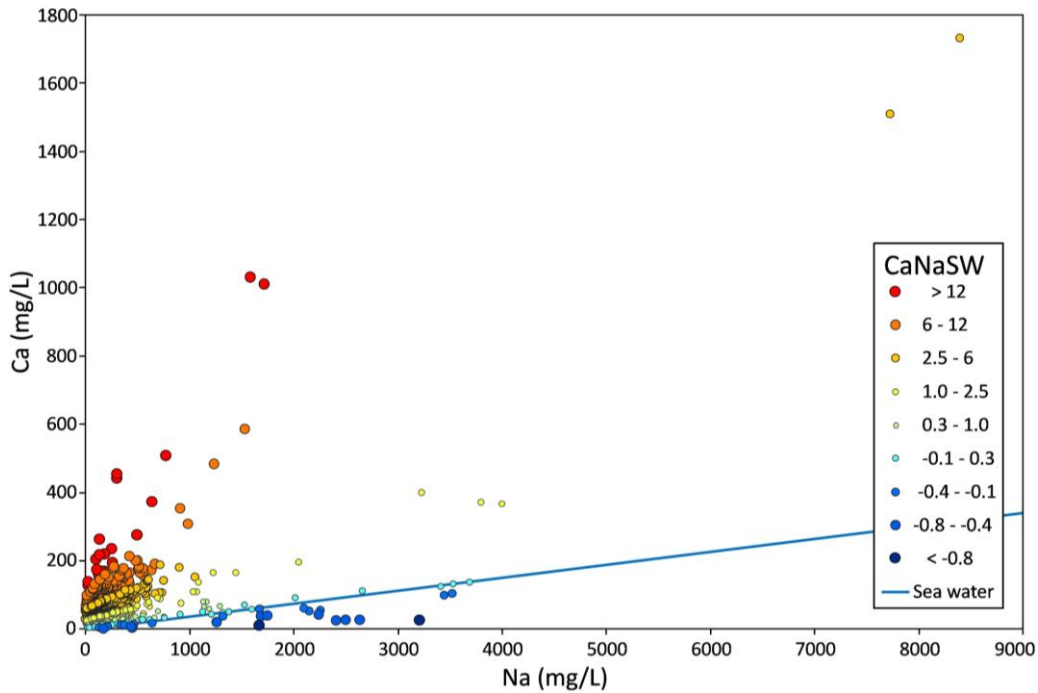


Figure 15: Dissolved Ca vs. Na for the corrected Stygo Pilbara groundwater dataset, coloured by the CaNaSW range.

5.2 Ion Excess or Deficit

Absolute differences in ion concentration relative to the sea water line (e.g. Figure 16) were calculated. In order to remove erroneous values in saline samples due to analytical error, deviations less than 10% from the sea water line gave a value of zero:

$$\begin{aligned}
 \mathbf{KNaDSW} &= K - (0.0399 \times Na) && \dots \mathbf{KNaSW} > 0.1 \\
 &= 0 && \dots -0.1 \leq \mathbf{KNaSW} \leq 0.1 \\
 &= K - (0.0327 \times Na) && \dots \mathbf{KNaSW} < -0.1 \\
 \\
 \mathbf{MgNaDSW} &= Mg - (0.1314 \times Na) && \dots \mathbf{MgNaSW} > 0.1 \\
 &= 0 && \dots -0.1 \leq \mathbf{MgNaSW} \leq 0.1 \\
 &= Mg - (0.1075 \times Na) && \dots \mathbf{MgNaSW} < -0.1 \\
 \\
 \mathbf{CaNaDSW} &= Ca - (0.0419 \times Na) && \dots \mathbf{CaNaSW} > 0.1 \\
 &= 0 && \dots -0.1 \leq \mathbf{CaNaSW} \leq 0.1 \\
 &= Ca - (0.0343 \times Na) && \dots \mathbf{CaNaSW} < -0.1 \\
 \\
 \mathbf{SO_4ClDSW} &= SO_4 - (0.1536 \times Cl) && \dots \mathbf{SO_4ClSW} > 0.1 \\
 &= 0 && \dots -0.1 \leq \mathbf{SO_4ClSW} \leq 0.1 \\
 &= SO_4 - (0.1256 \times Cl) && \dots \mathbf{SO_4ClSW} < -0.1
 \end{aligned}$$

Comparing the Ca:Na difference (Figure 16) with the ion ratio parameter differentiation (Figure 15) indicates how the ion ratio and ion difference parameters differentiate the data in different manners.

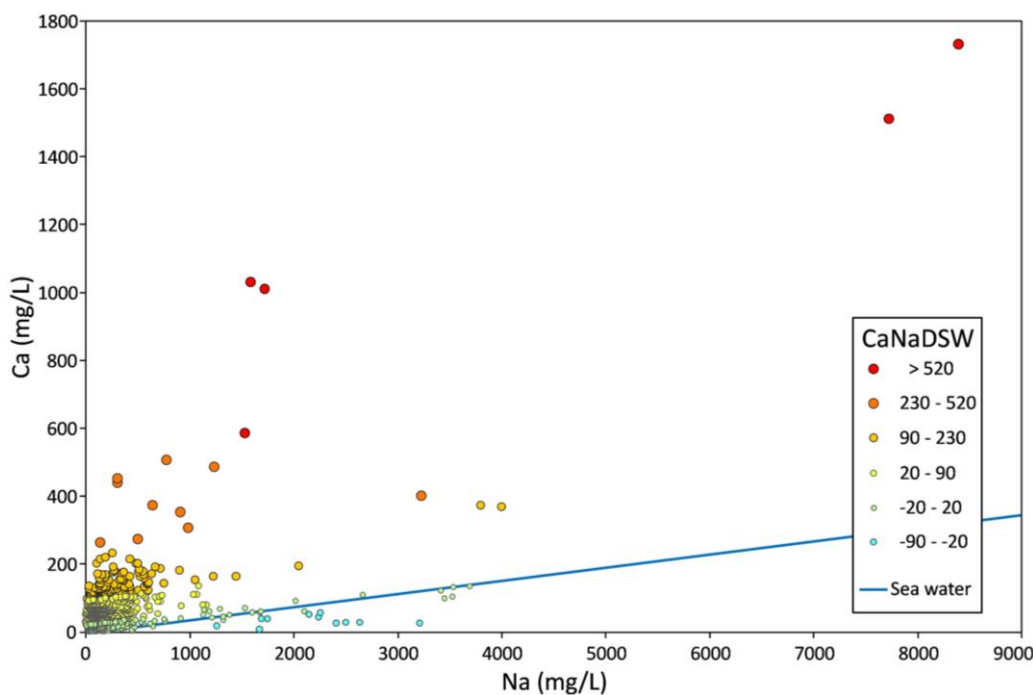


Figure 16: Dissolved Ca vs. Na for the corrected Stygo Pilbara groundwater dataset, coloured by the CaNaDSW range.

6 Solution Modelling

6.1 Activity Plots

Plotting the Eh/pH data for Stygo Pilbara groundwaters on the crystalline Fe mineral stability plot (Figure 17; derived using The Geochemist's Workbench®) indicates that these groundwaters are generally within the stability field for hematite (Fe_2O_3), although a few (< 10) waters are sufficiently reduced to sit near the hematite-pyrite (FeS_2) stability interface. It was previously noted there is a probable error in Eh measurements of 100 – 200 mV; though significant for calculations, this is minor for these plots (Eh axis has a range of 2000 mV; Figure 17).

However, groundwater Fe concentrations are commonly much higher than expected for crystalline Fe oxide solubility waters, and are commonly in equilibrium with amorphous forms of Fe (Schwab and Lindsay, 1983) such as ferrihydrite [$\text{Fe}(\text{OH})_3 \cdot x\text{H}_2\text{O}$] or $\text{Fe}_3(\text{OH})_8$. With crystalline Fe oxides removed from the modelling (Figure 18), most groundwaters sit within amorphous $\text{Fe}(\text{OH})_3$ or siderite (FeCO_3) fields, although the most acid (< pH 6) and reducing waters sit at the interface with soluble Fe^{2+} . Such modelling for Fe, and for other elements such as Mn, can assist in understanding element mobilities.

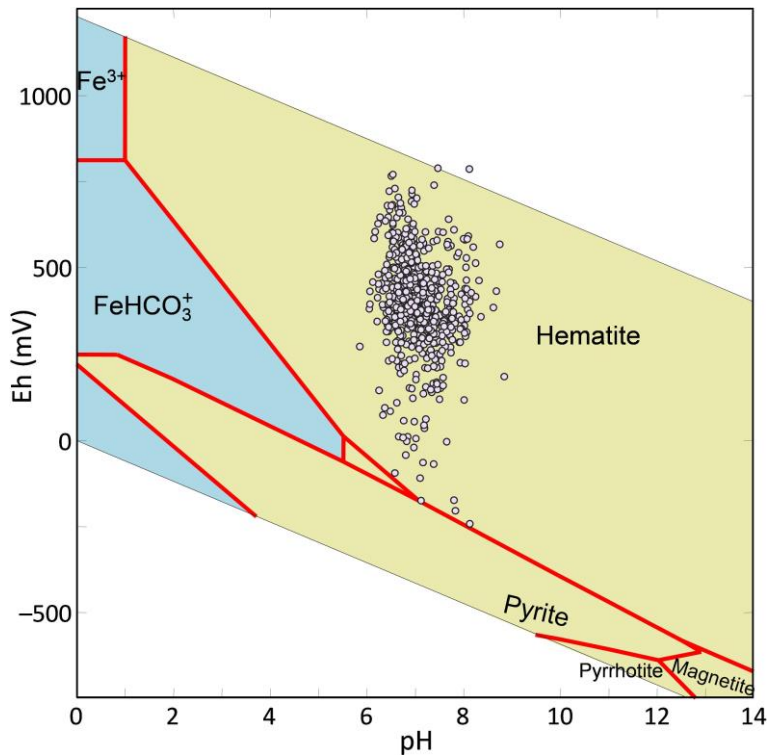


Figure 17: Modelled Eh-pH plot of Fe speciation overlain with Eh:pH data for the corrected Stygo Pilbara groundwaters. Blue zones denote where Fe is soluble and yellow zones where Fe will precipitate as the mineral shown. Solution activities used in the modelling are 10^{-4} M Fe, 0.01M S, 1% CO_2 fugacity, hematite suppressed, $25^\circ\text{C}/1.013$ bars. (Geochemists Workbench®, thermo.dat database).

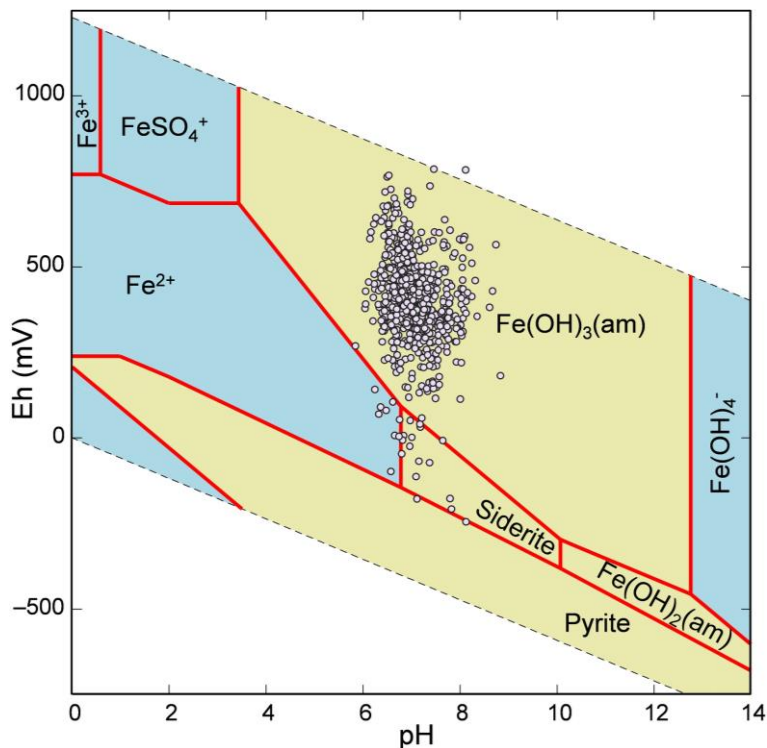


Figure 18: Modelled Eh-pH plot of Fe speciation (crystalline Fe oxides not involved) overlain with Eh:pH data for the corrected Stygo Pilbara groundwaters. Blue zones denote where Fe is soluble and yellow zones where Fe will precipitate as the mineral shown. Solution activities used in the modelling are 10^{-4} M Fe, 0.01M S, 1% CO_2 fugacity, hematite, goethite, magnetite, FeO, and troilite suppressed, $25^\circ\text{C}/1.013$ bars. (Geochemists Workbench®, thermo.dat database).

6.2 Mineral Saturation Indices

Solution chemical speciation and degree of mineral saturation were computed from the solution compositions using the program PHREEQE (Parkhurst et al., 1980). Saturation indices (SI) for each water sample were calculated for various minerals. If the SI for a mineral is within the zero range, then the water is in equilibrium with that mineral, under the conditions specified. The zero range is estimated for every mineral based on stoichiometry, thermodynamic accuracy and analytical issues; generally ranging from -0.2 to 0.2 for major element minerals such as gypsum (Figure 19) to -1 to 1 for minor element minerals. Where

the SI is below the zero range, the solution is under-saturated with respect to that mineral, so that, if present, the phase may dissolve. If the SI is greater than zero the solution is over-saturated with respect to this mineral, which could potentially precipitate from solution.

Note that SI determinations only specify possible reactions, and kinetic constraints may rule out reactions that are thermodynamically allowed. Thus, for example, waters are commonly close to equilibrium with respect to carbonate minerals such as calcite (Figure 20), but may become dolomite over-saturated, due to the slow rate of precipitation of this mineral (Drever, 1982). However, this method provides some understanding of solution processes at a site and adds value in determining whether the spatial distribution of an element is correlated with geological phenomena such as lithology or mineralisation, or whether solubility is related to weathering or environmental effects. For example, if Ca distribution is controlled by equilibrium with gypsum in particular samples (Figure 19), then the spatial distribution of dissolved Ca will reflect SO₄ concentration alone and have no direct exploration significance.

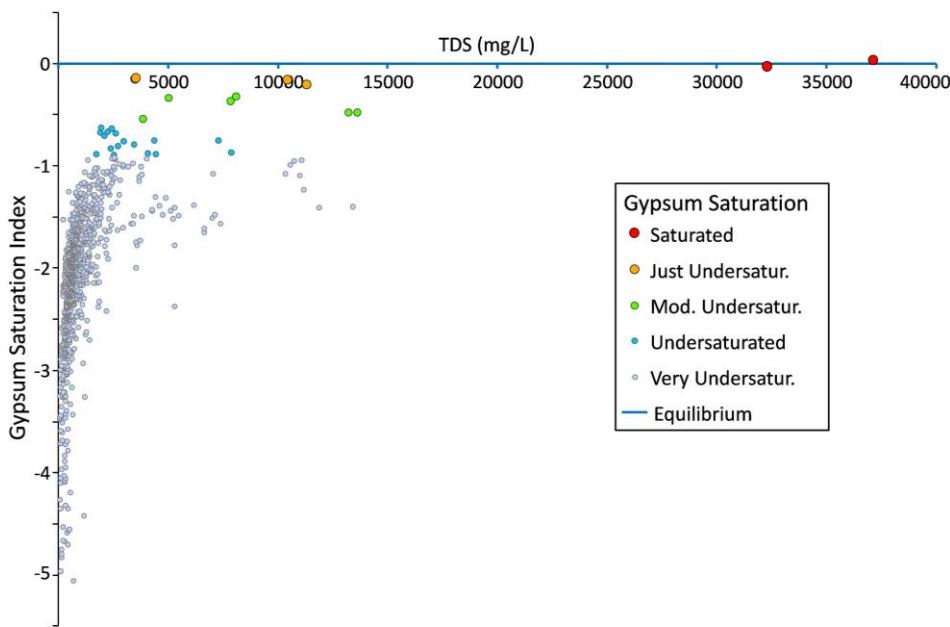


Figure 19: Gypsum Saturation Index (SI) vs. TDS for the corrected Stygo Pilbara groundwater dataset, grouped by the defined saturation level.

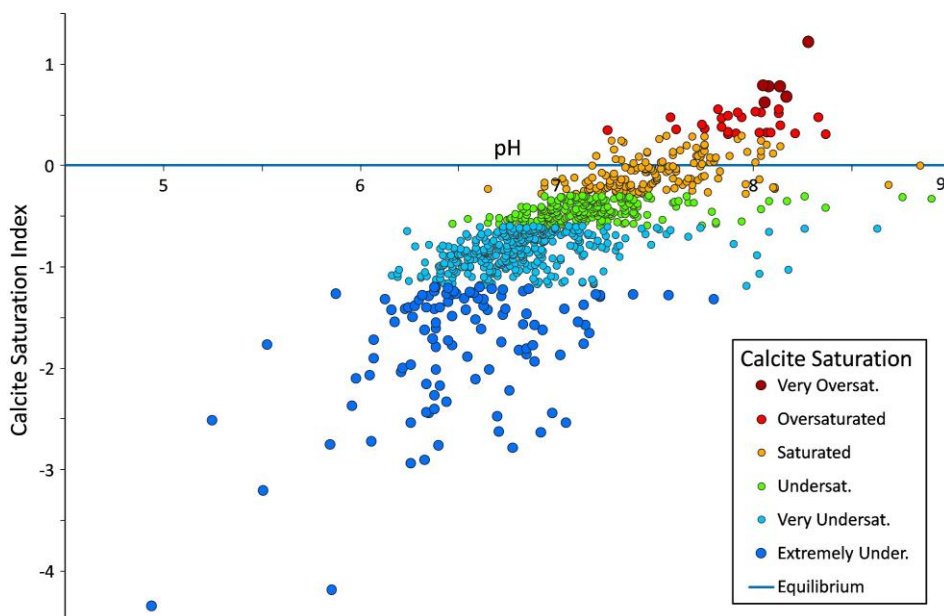


Figure 20: Calcite Saturation Index (SI) vs. pH for the corrected Stygo Pilbara groundwater dataset, grouped by the defined saturation level.

7 Some Results

The Stygo Pilbara hydrogeochemical dataset is available online (Gray, 2016a; <http://doi.org/10.4225/08/575CDF639A59A>). This section shows some examples of the groundwater data set mapped for regional analysis, in conjunction with other data (Figure 1). This is meant to give a general flavour for the utility of this dataset. It is expected that further research will be conducted on optimising this data for geological mapping, prospectivity analysis, environmental baselines and other uses.

The Archaean-aged Pilbara Craton has a complex geology, overlain with weathering alteration. Completing the groundwater map of the region should assist in discriminating various geological regions. Two major controlling factors in groundwater are salinity (Figure 21) and pH (Figure 22). Pilbara groundwaters tend to be fresh (Figure 21), relative to much of the rest of Australia, though moderate salinities are observed close to the coast and in the main palaeo-channel system. Similarly, Pilbara groundwaters have low acidity, generally close to pH 7 (Figure 22), although lower pH values are observed in the Ashburton (directly south of the Pilbara) and Wittenoom Formations.

Ion ratios (Section 5.1), identify deviations from the sea water line for ion pairs. Thus, for example, using the MgNaSW index (Figure 23), the Eromanga Basin is clearly identified at the continental scale by the prevalent low Mg:Na ratio. Variation in Mg:Na is more gradational in WA, although there is a subtle increase in Mg:Na in groundwaters from greenstones, relative to granites, in the northern Yilgarn Craton. The Pilbara Craton is characterised by higher Mg:Na (Figure 23), though with some of the specific sub-units having lower Mg:Na. Similar observations can be made for the CaNaSW index (Figure 24), although with differing internal variations within the Pilbara. Using ion excess calculations (Section 5.2), this high Ca:Na ratio is indicated to be a significant Ca enrichment (Figure 25).

In contrast, the strongest features delineated in a continental map of the KNaSW index (Figure 26), are high K:Na groundwaters in the NE Yilgarn Craton and various shield rocks of in central Australia. Within the Pilbara, there are major K:Na differences between different rock types. Using the ion excess (KNaDSW) index (Figure 27), some of these units, most notably the Wittenoom Formation, appear to have high absolute K relative to Na. The SrCaSW Index (Figure 28), as in the northern Yilgarn Craton (Gray et al., 2016), also shows value for rock discrimination in the Pilbara, particularly in conjunction with the other Indices discussed above.

The SO₄ClSW Index (Figure 29) shows high SO₄:Cl across much of central WA and Australia. For parts of this central Australian zone where high SO₄:Cl (Figure 29) correlates with waters at or near gypsum (CaSO₄.H₂O) saturation (Figure 30), this suggests S dissolving into the groundwaters, possibly from gypsum itself, with possible other sources including oxidation of sulfides. Even fewer areas within the Pilbara are close to celestine (SrSO₄) saturation (Figure 31).

Both dissolved Si and calculated silica saturation (Figure 32), are highly related, with silica saturation maps giving very good contrast for mapping. The Shield rocks of the Musgraves, Yilgarn and Pilbara all show high dissolved Si and commonly reach silica saturation (Figure 32). The smaller zones of silica undersaturation in these areas may represent specific processes, which require further research. In contrast, the Pilbara Craton has much lower dissolved NO₃ (Figure 33) and total N concentrations than the Capricorn Orogen and Yilgarn Craton to the south. Calculated saturation indices for carbonate minerals such as calcite (Figure 34), dolomite or magnesite gave highly variable mapping, possibly suggesting localised controls and/or high errors in pH measurement.

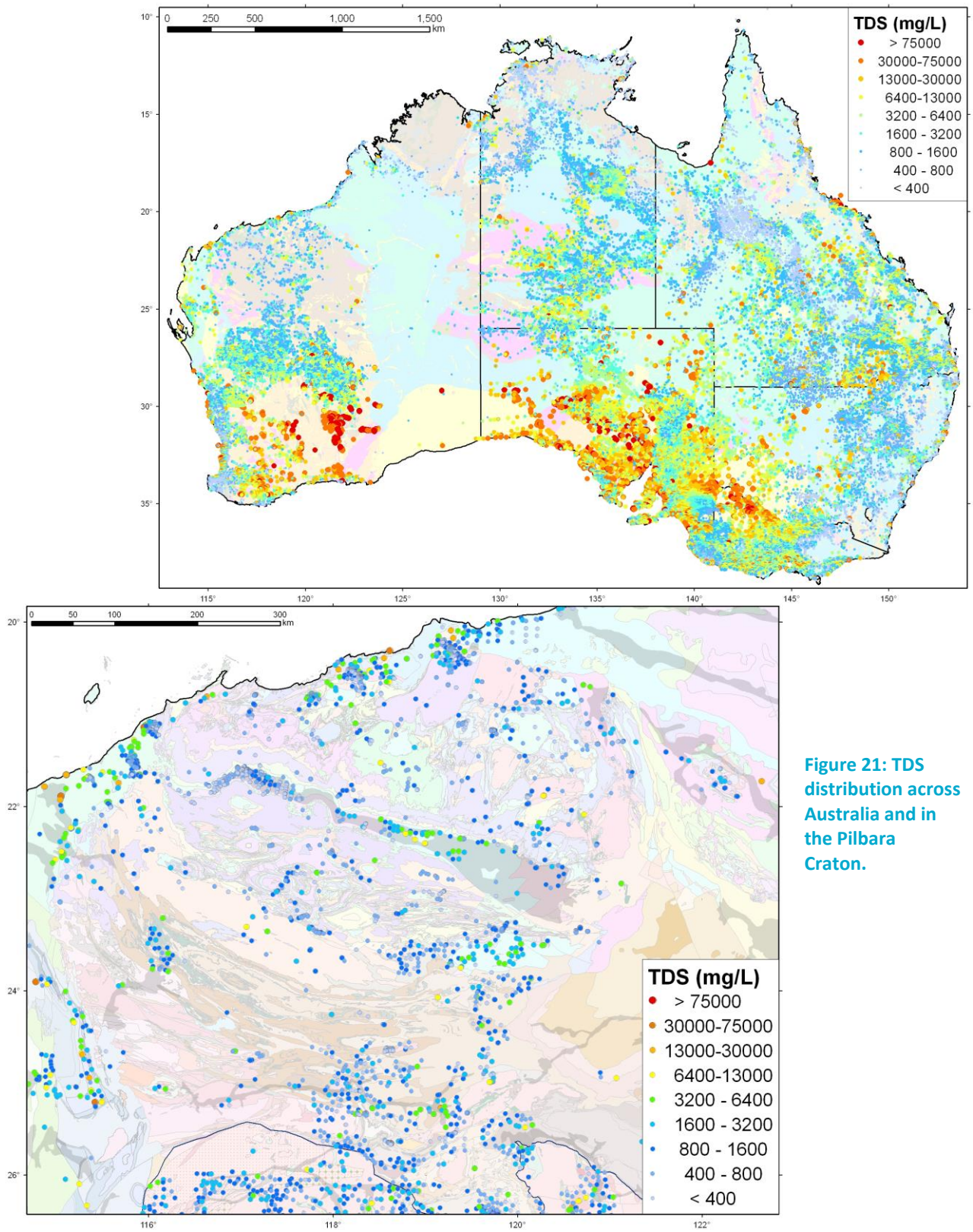


Figure 21: TDS distribution across Australia and in the Pilbara Craton.

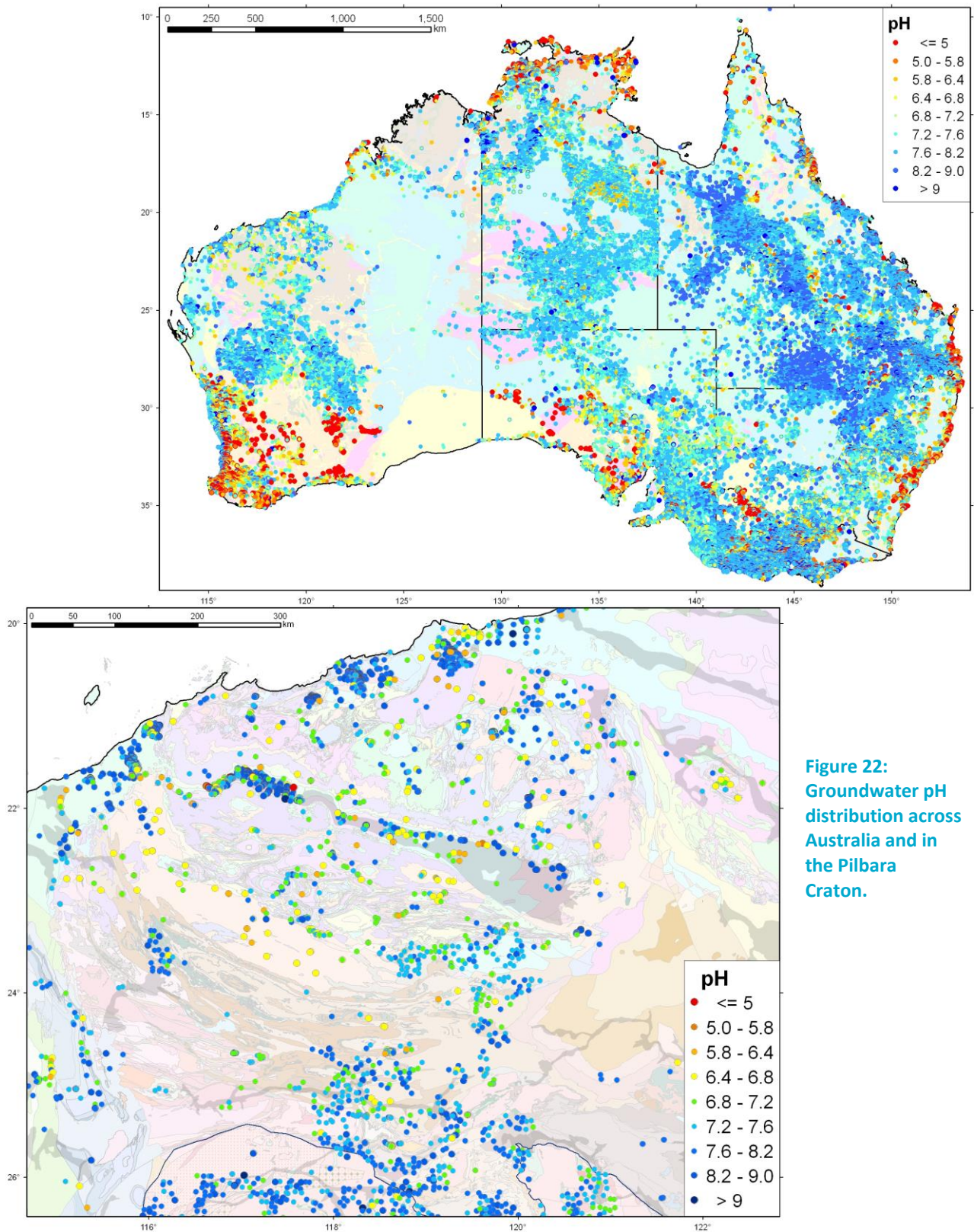


Figure 22:
Groundwater pH
distribution across
Australia and in
the Pilbara
Craton.

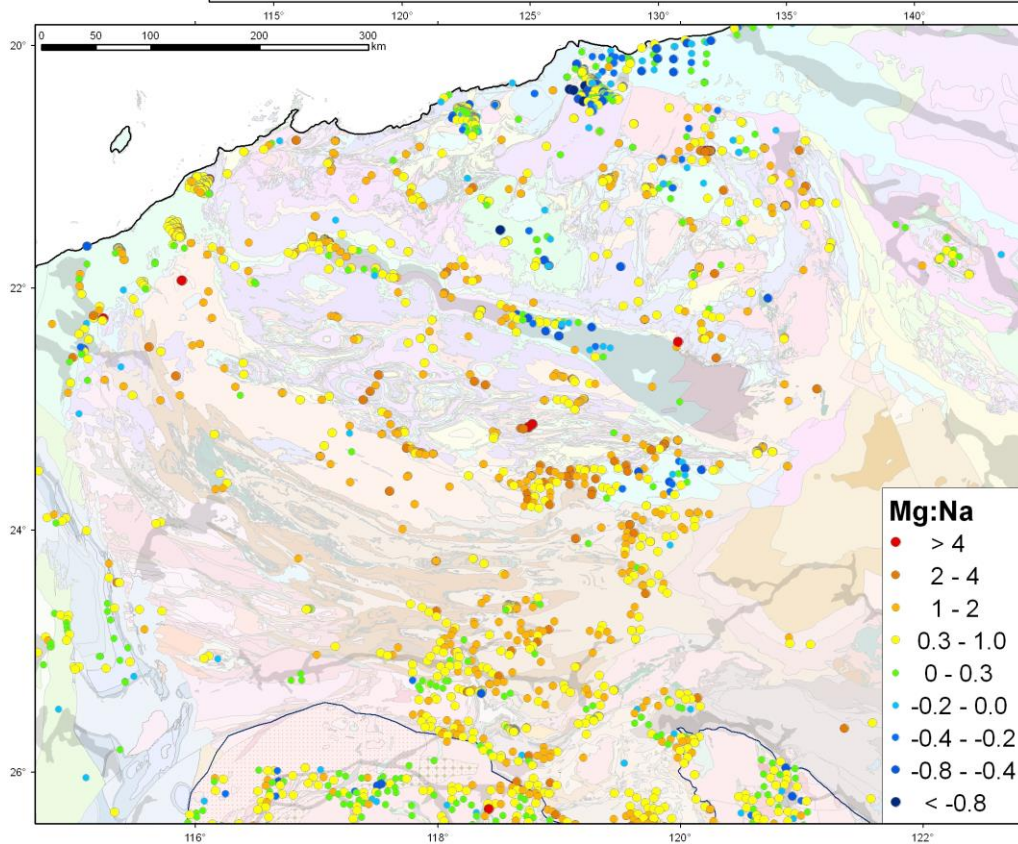
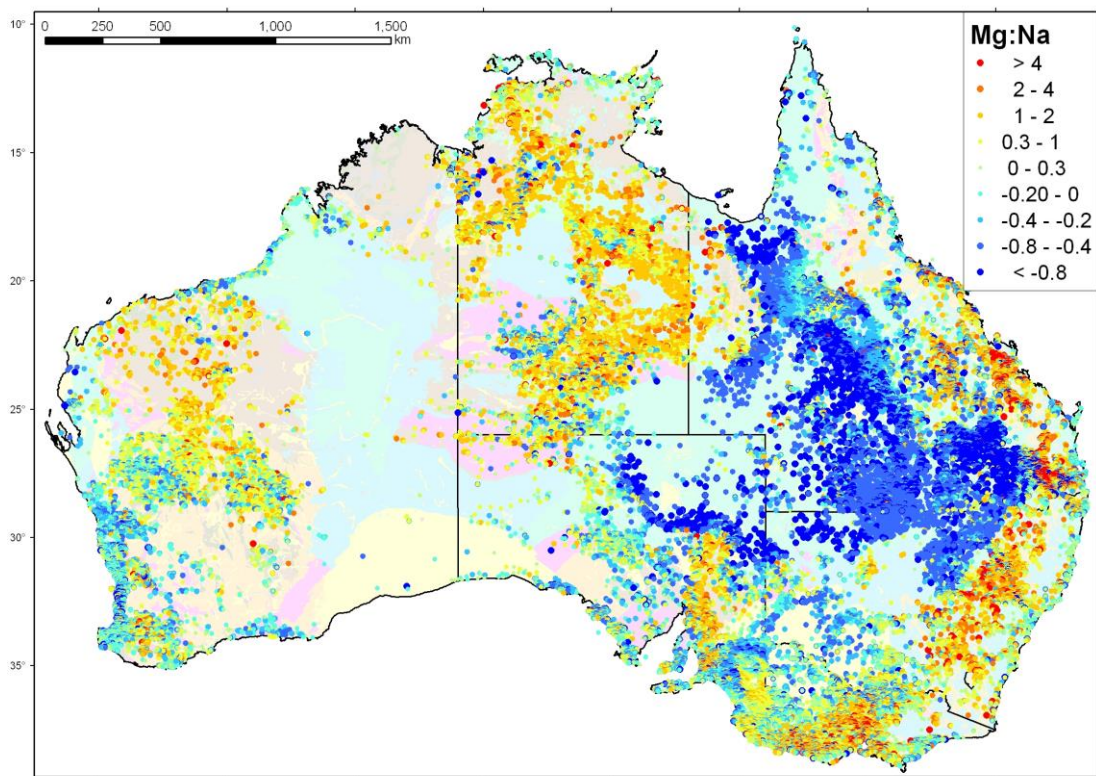


Figure 23:
Groundwater
Mg:Na Ion Ratio
(MgNa_{SW})
distribution across
Australia and in
the Pilbara
Craton.

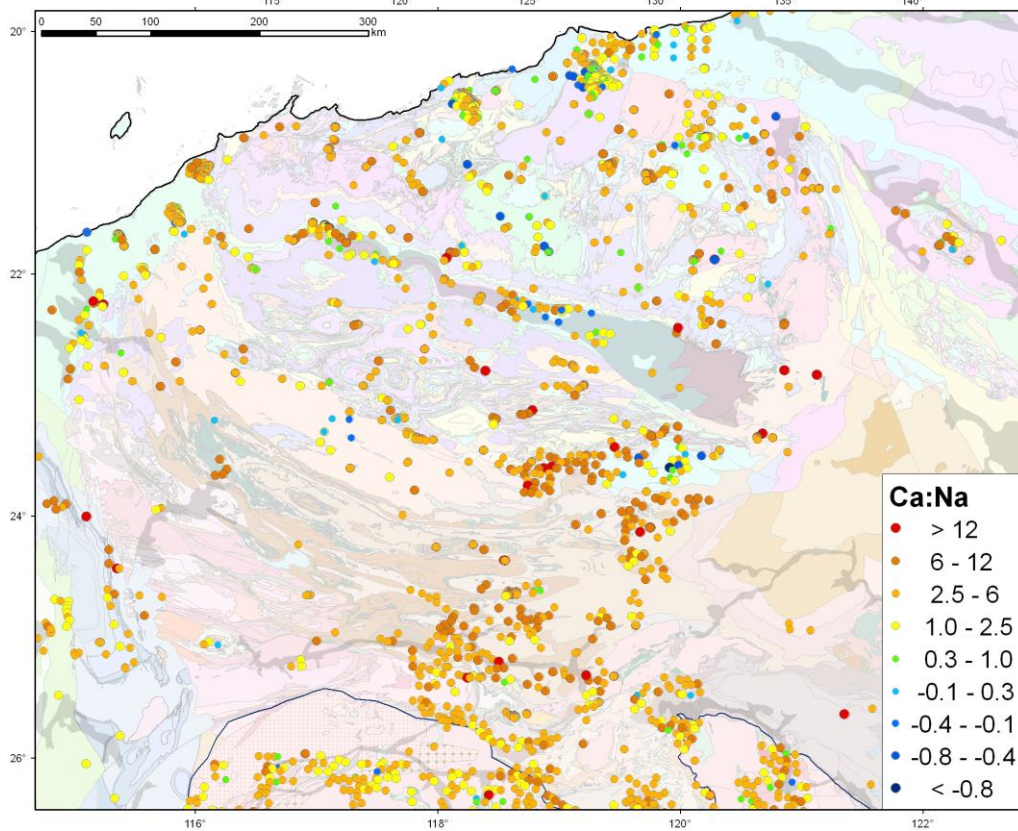
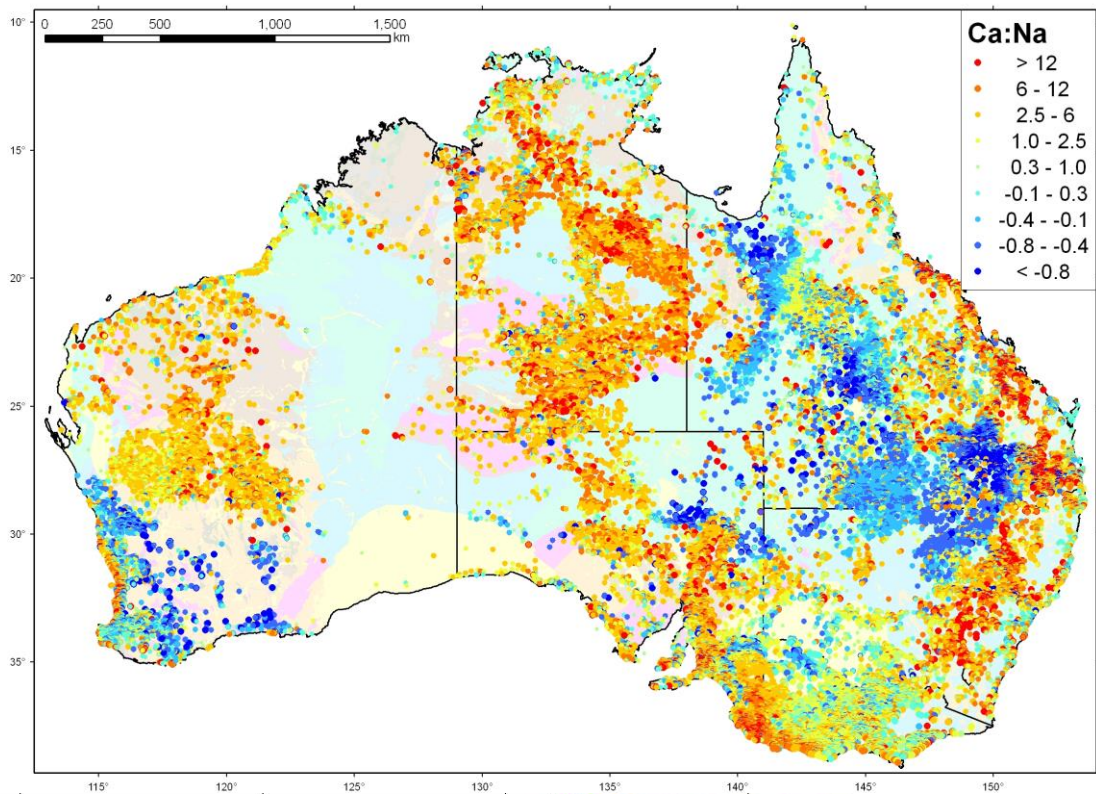


Figure 24:
Groundwater
Ca:Na Ion Ratio
(CgNaSW)
distribution across
Australia and in
the Pilbara
Craton.

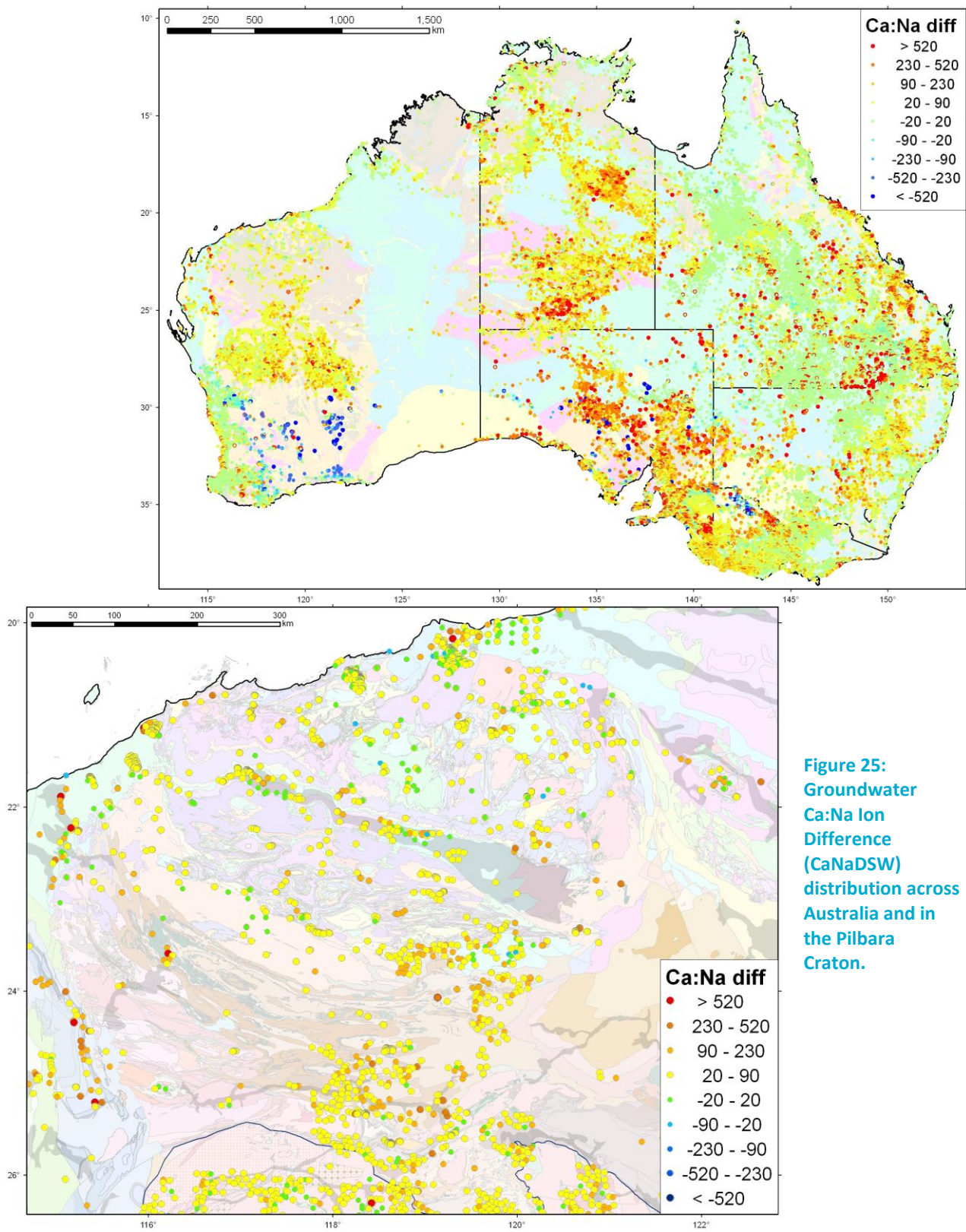


Figure 25: Groundwater Ca:Na Ion Difference (CaNaDSW) distribution across Australia and in the Pilbara Craton.

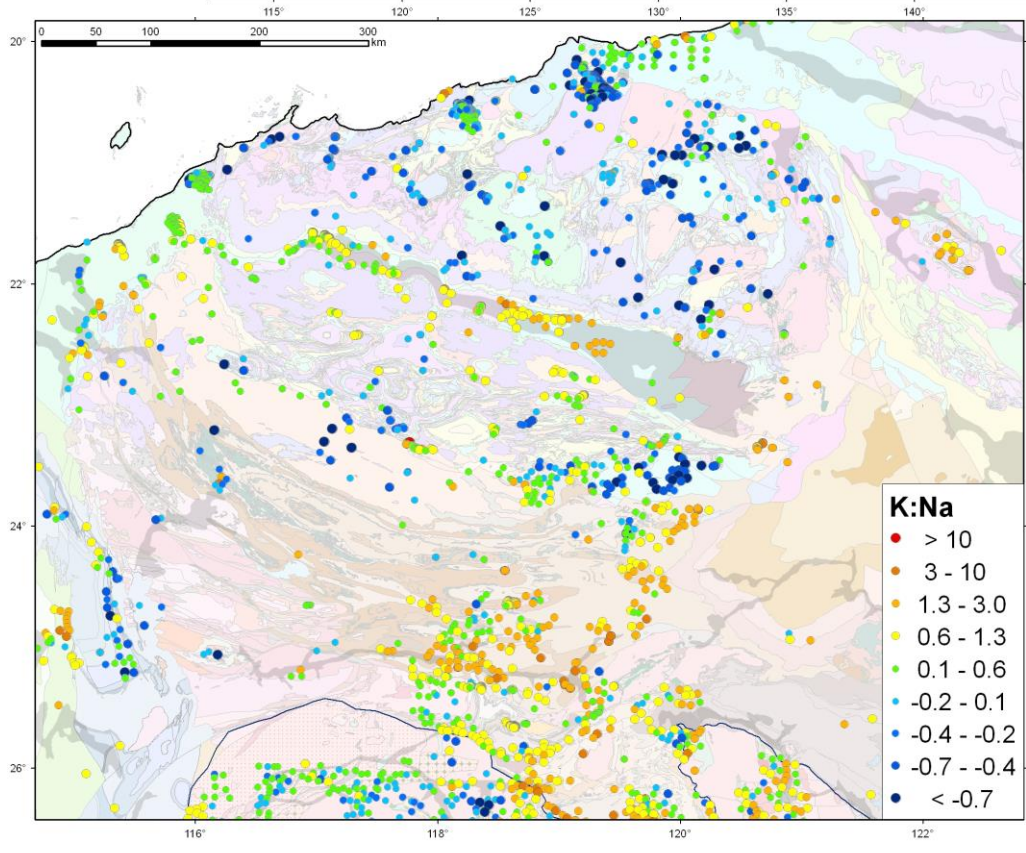
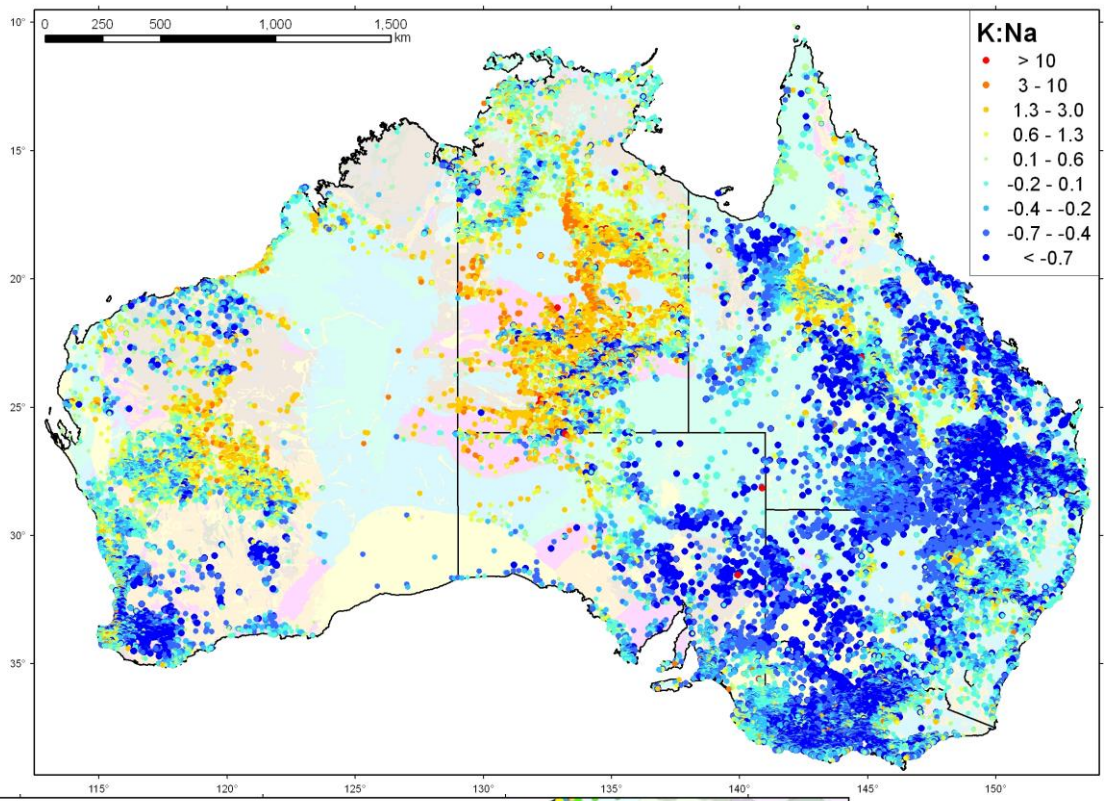


Figure 26:
Groundwater
K:Na Ion Ratio
(KNaSW)
distribution across
Australia and in
the Pilbara
Craton.

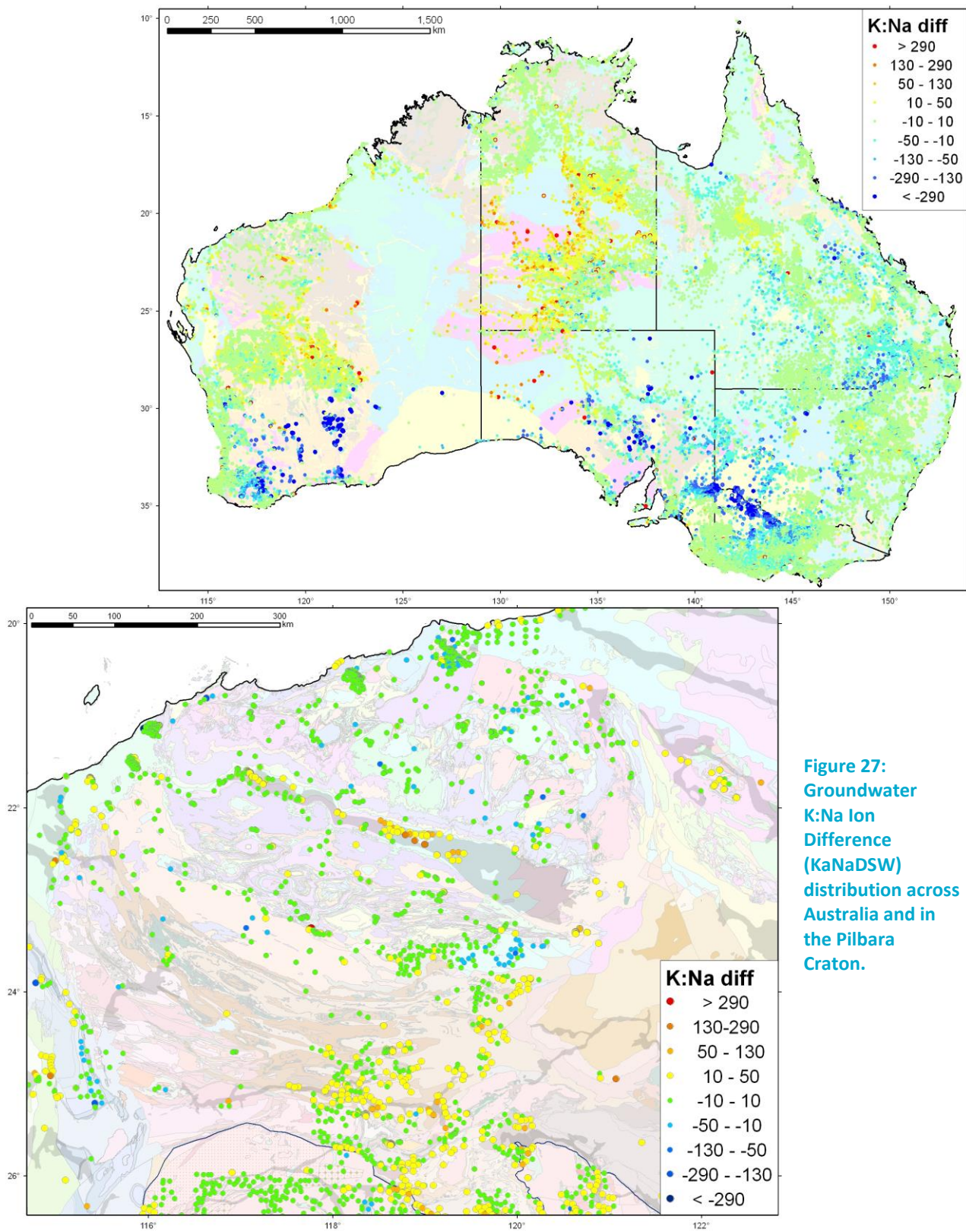


Figure 27:
Groundwater
K:Na Ion
Difference
(KaNaDSW)
distribution across
Australia and in
the Pilbara
Craton.

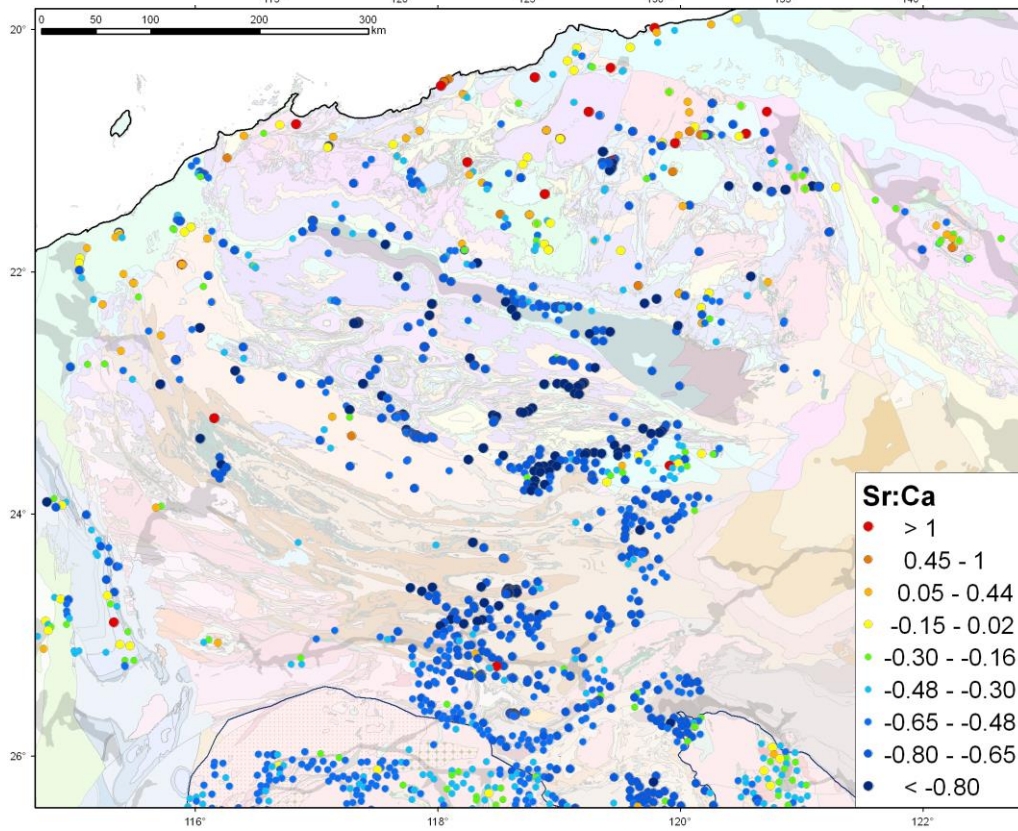
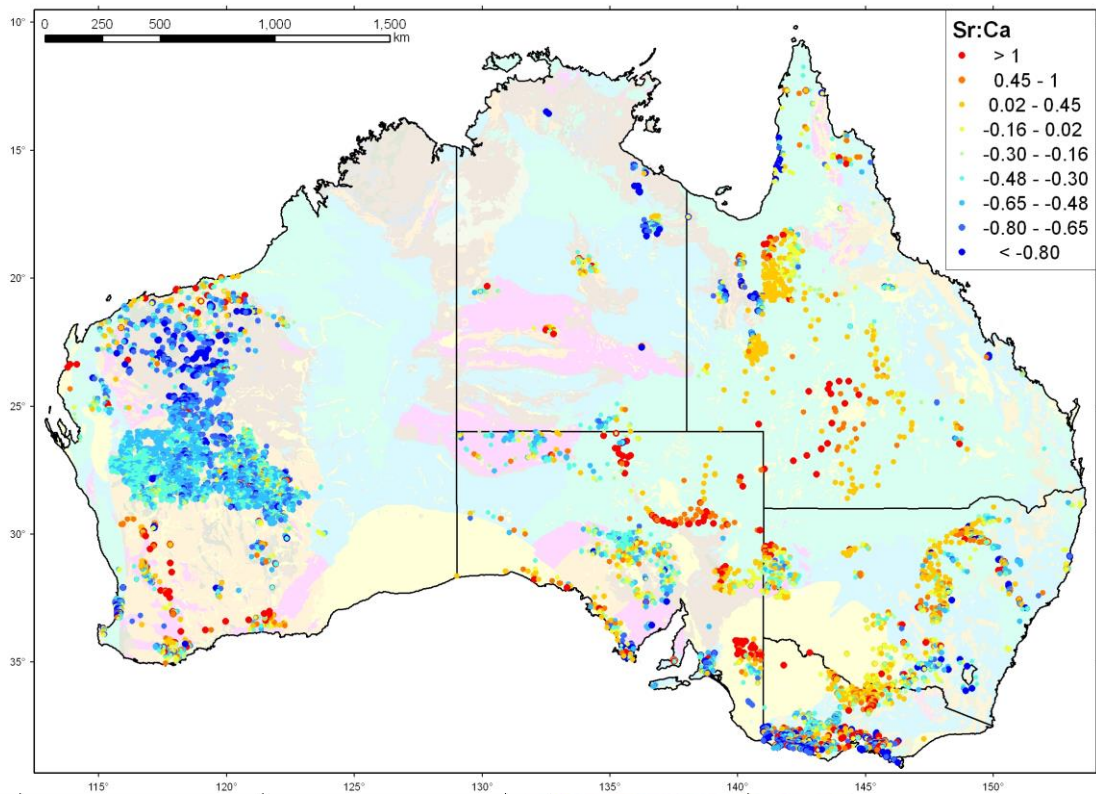


Figure 28:
Groundwater
Sr:Ca Ion Ratio
(SrCaSW)
distribution across
Australia and in
the Pilbara
Craton.

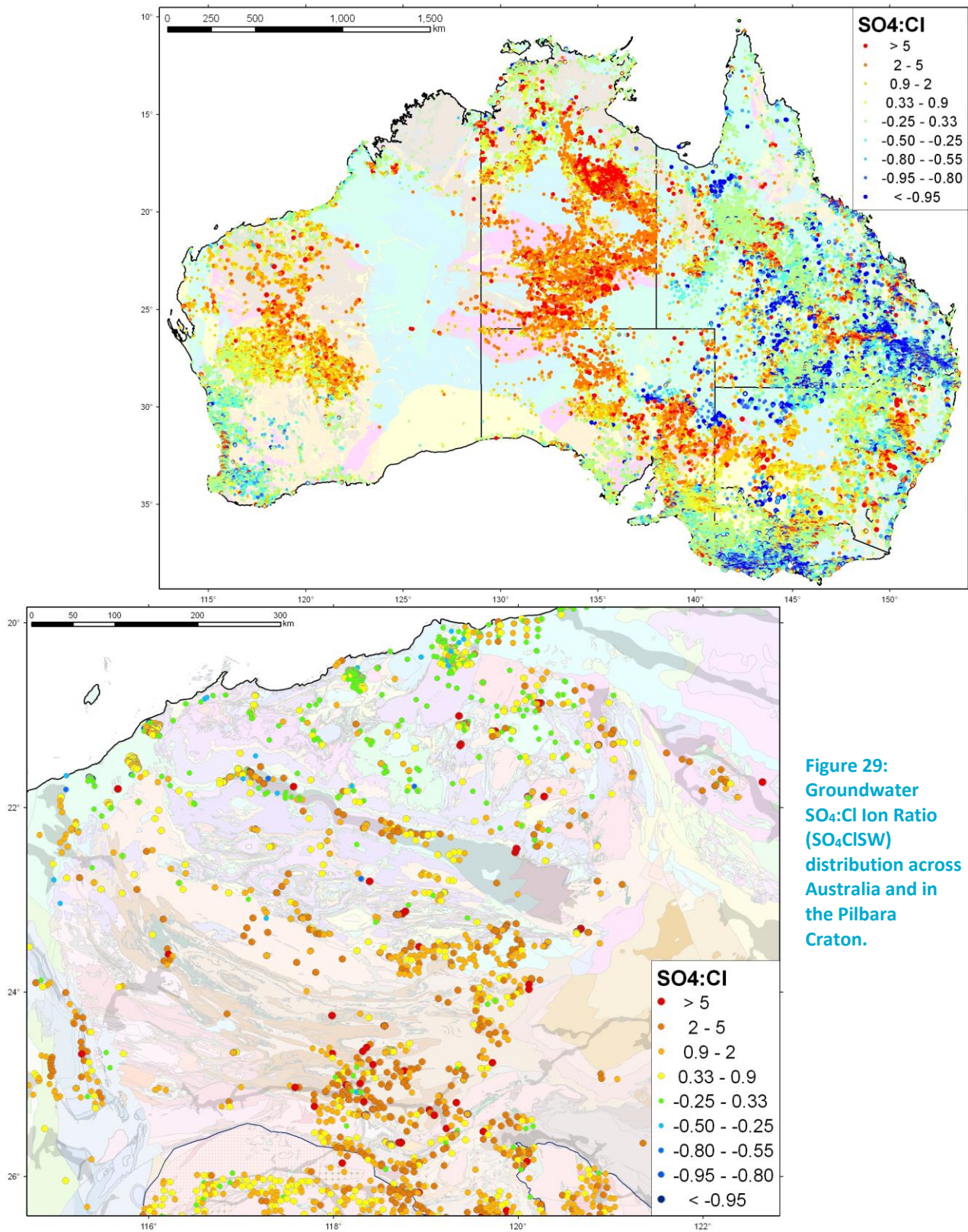


Figure 29:
Groundwater
SO₄:Cl Ion Ratio
(SO₄ClSW)
distribution across
Australia and in
the Pilbara
Craton.

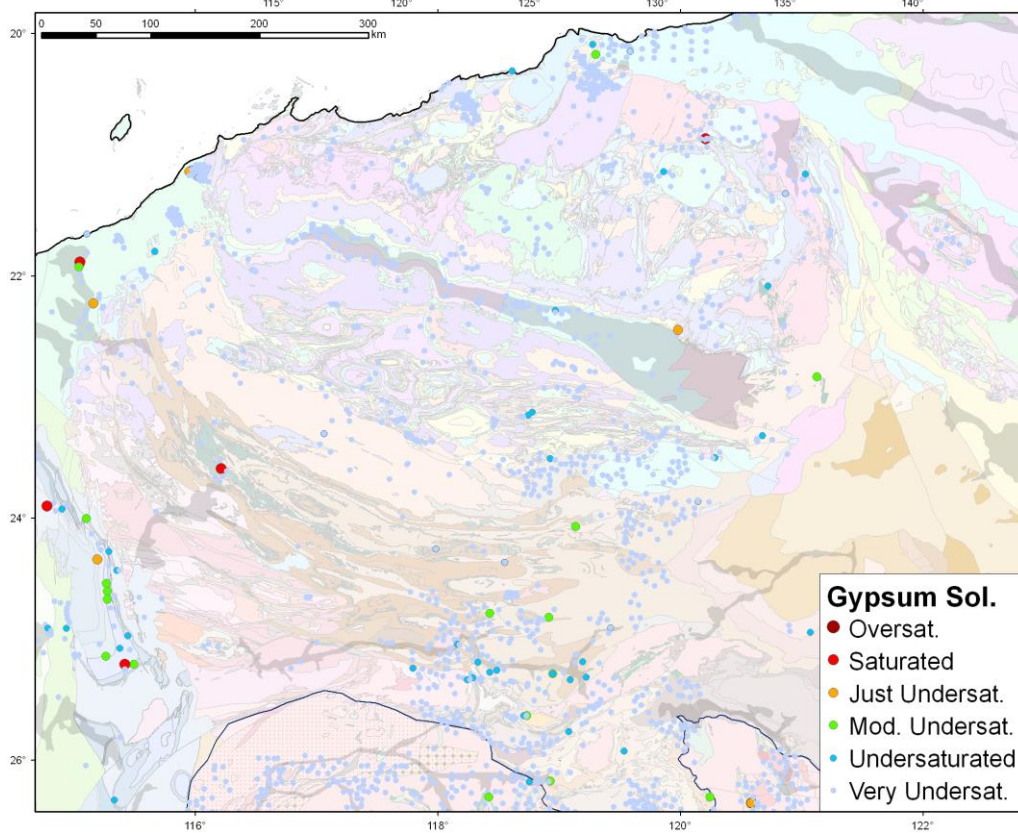
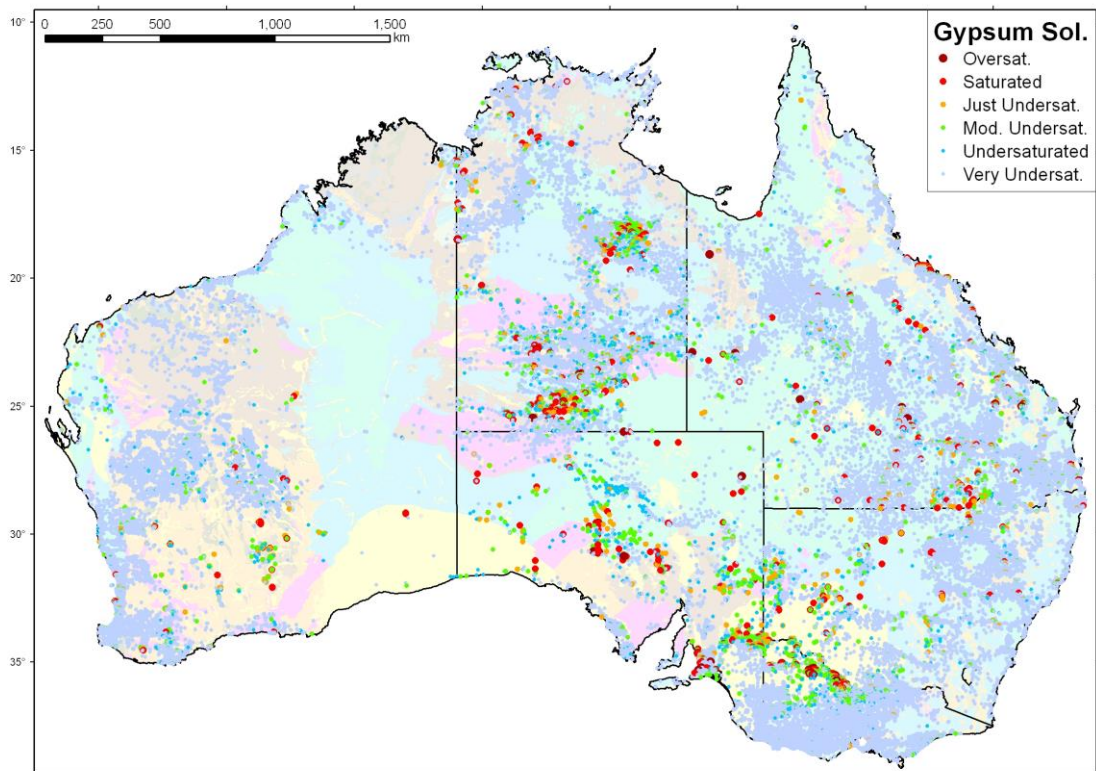


Figure 30:
Groundwater
gypsum saturation
distribution across
Australia and in
the Pilbara
Craton.

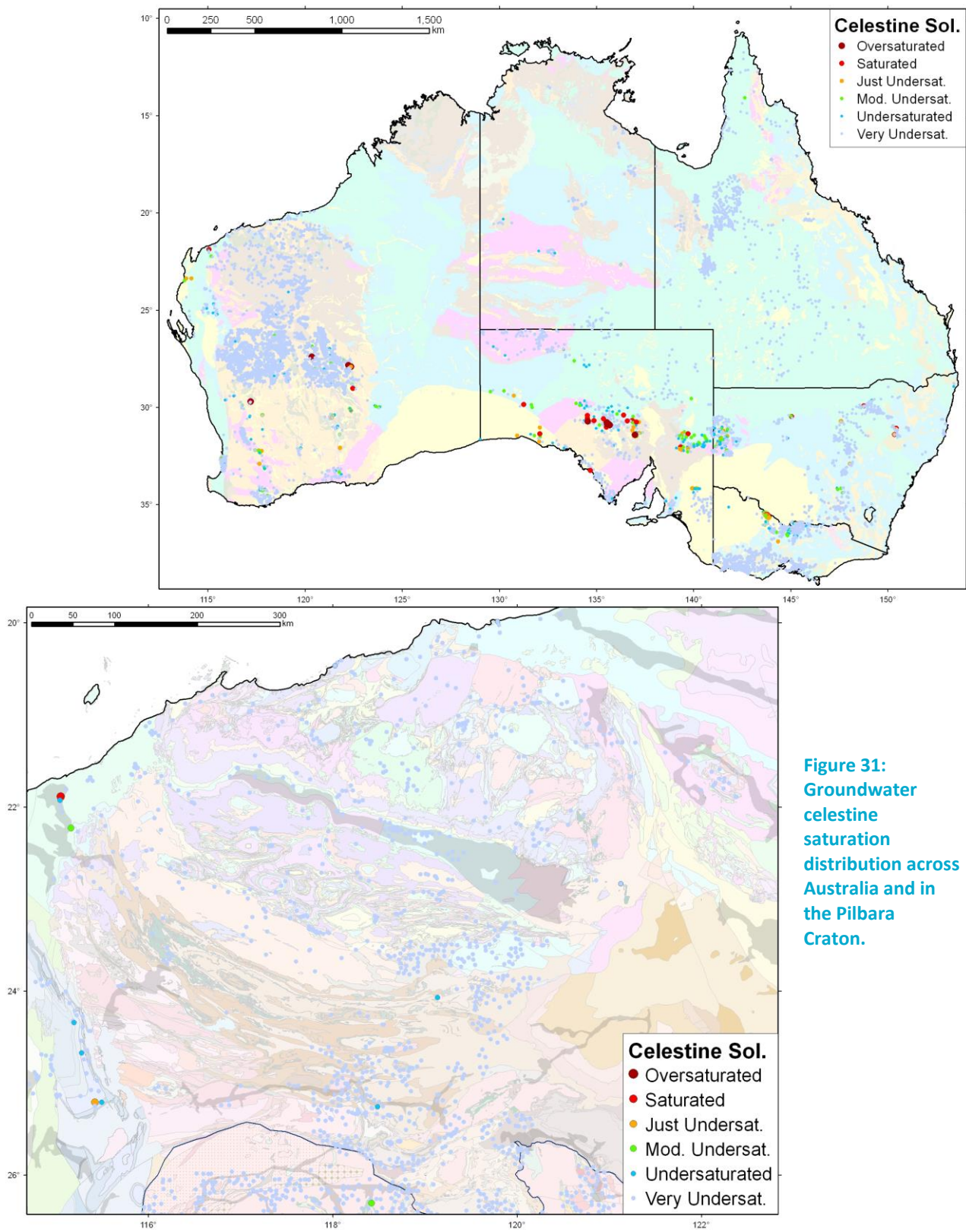


Figure 31:
Groundwater
celestine
saturation
distribution
across
Australia
and in
the Pilbara
Craton.

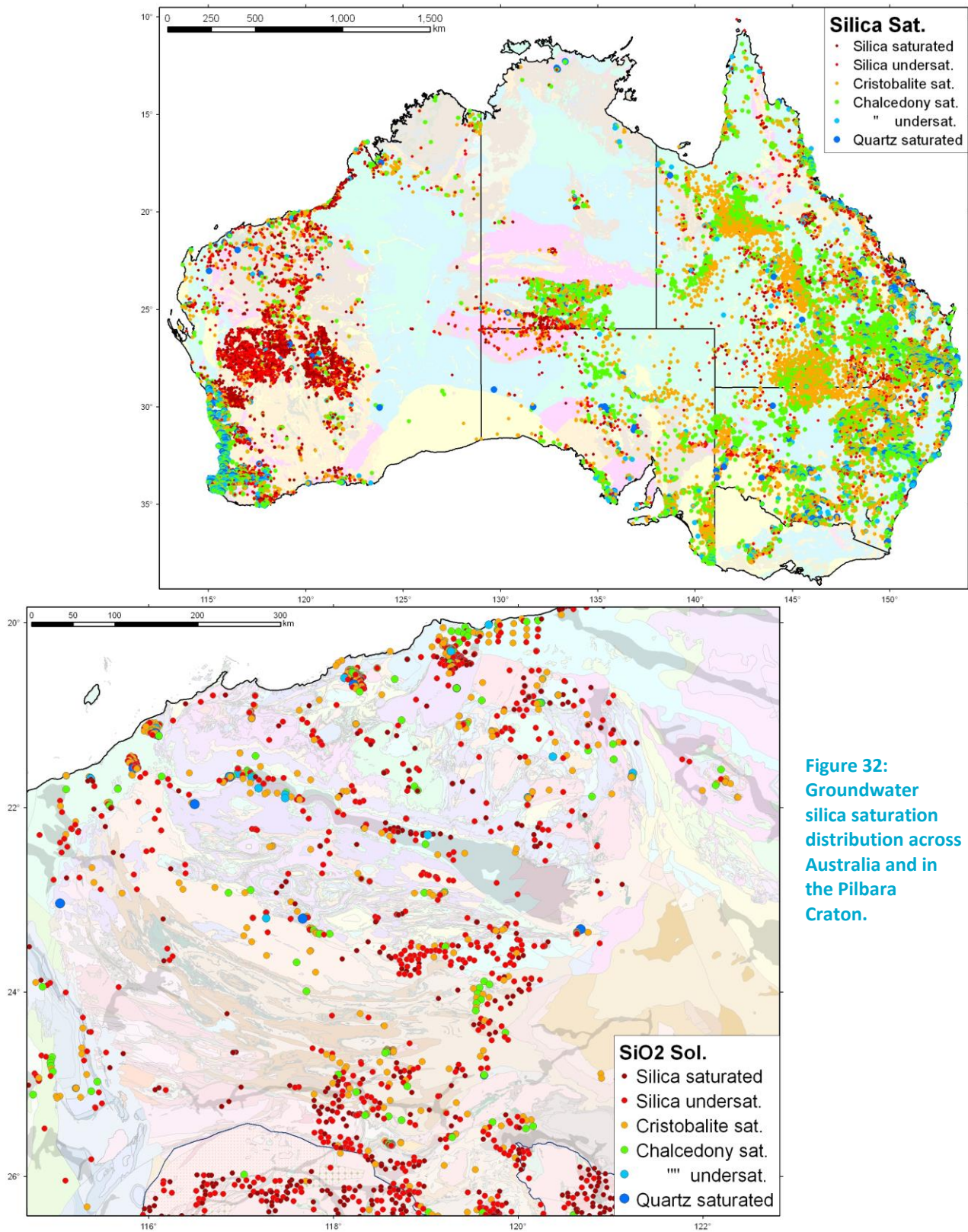


Figure 32:
Groundwater
silica saturation
distribution across
Australia and in
the Pilbara
Craton.

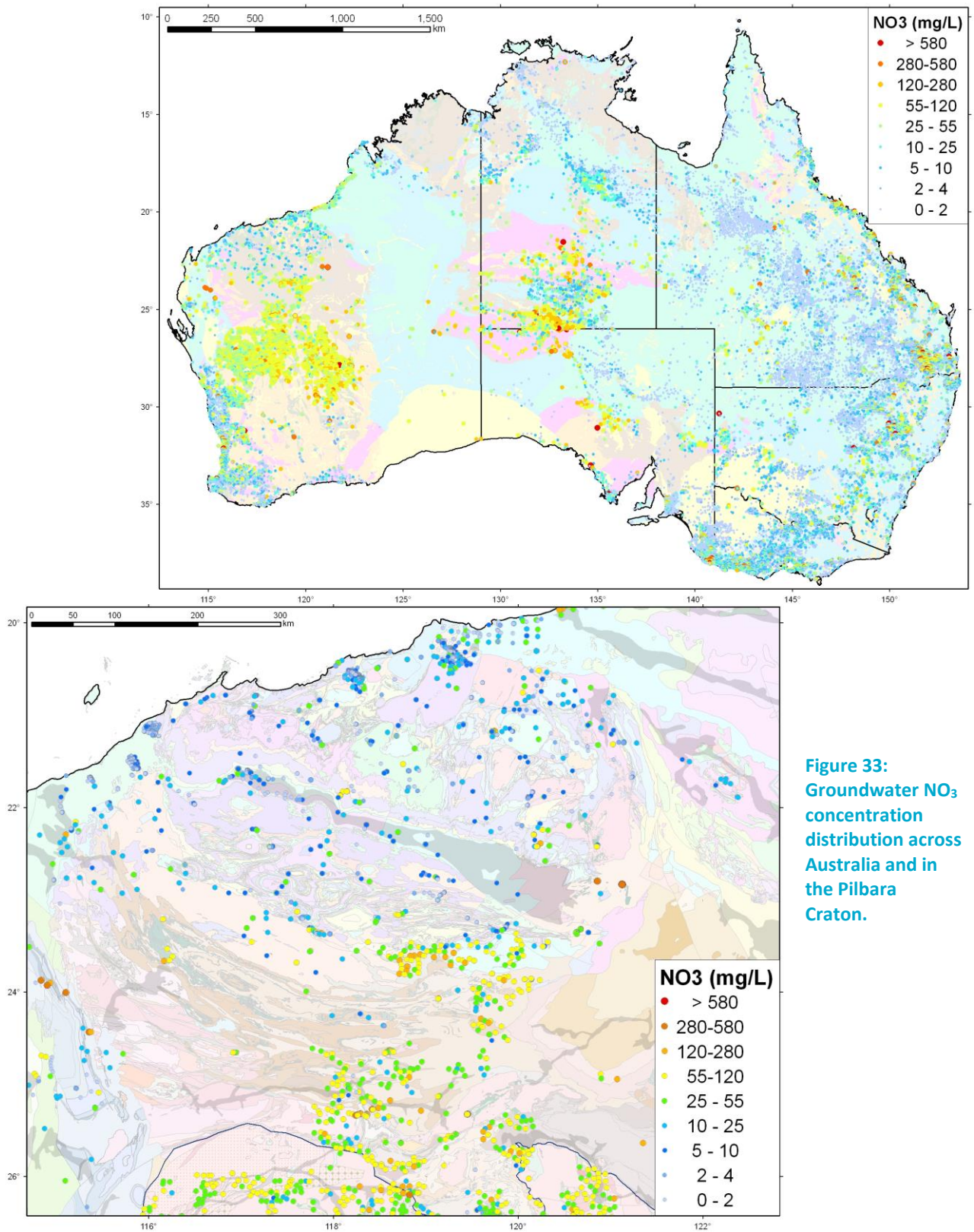
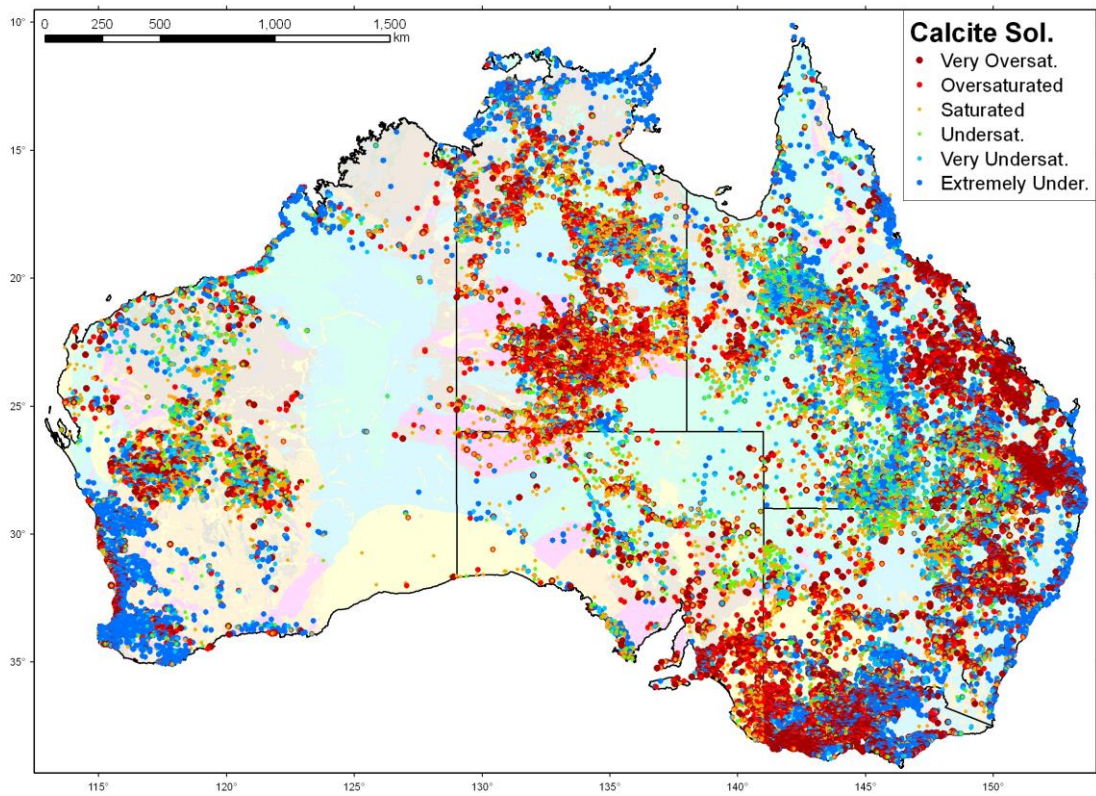


Figure 33:
Groundwater NO₃
concentration
distribution across
Australia and in
the Pilbara
Craton.



5

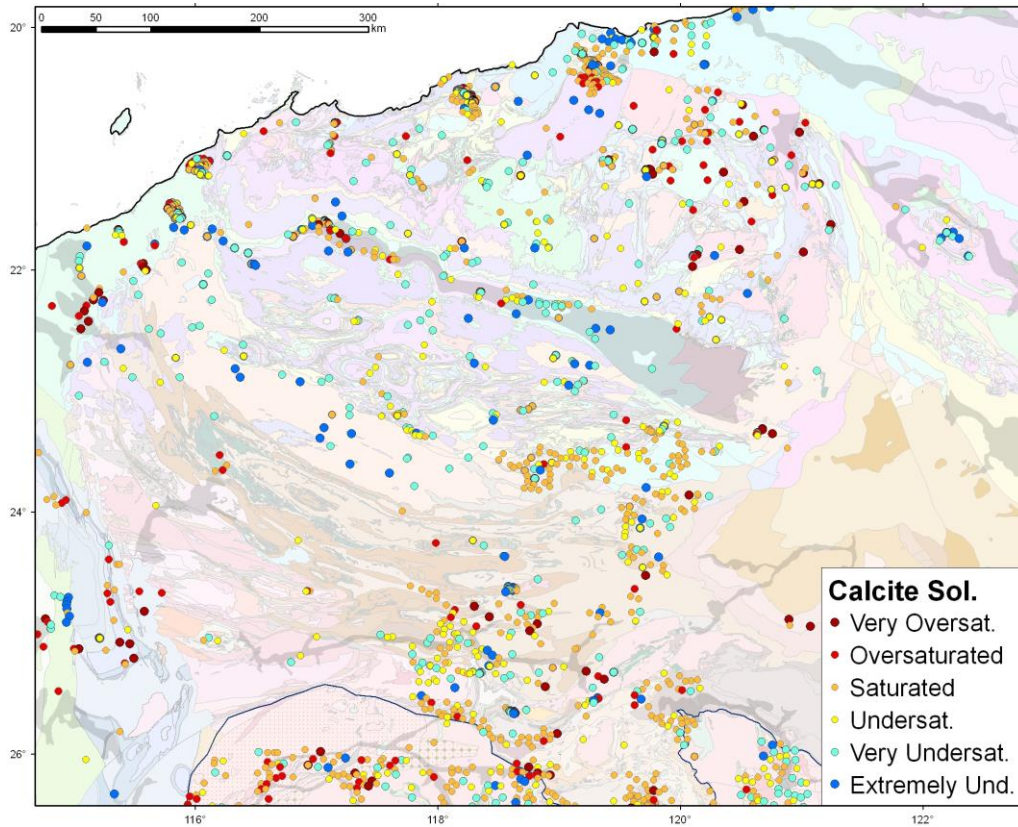


Figure 34:
Groundwater
Calcite saturation
distribution across
Australia and in
the Pilbara
Craton.

8 Conclusion

As part of the Continental Scale Hydrogeochemistry initiative (Figure 1), useful groundwater datasets from other researchers are being integrated with CSIRO sampling, so as to optimise the utility of groundwater geochemistry for mapping processes and geology across Australia. The Stygo Pilbara groundwater dataset contributed by Bennelongia Environmental Consultants was therefore subject to a thorough QA/QC assessment. Data that did not pass the assessment was rejected. Erroneous data (from well contamination and/or analytical or transcribing errors) have been minimised and data appears coherent, with seamless geochemical mapping across datasets.

Utilising this information, this dataset is being combined with other dataset, to map the groundwater chemistry of major geological regions within Australia. Deriving relatively simple parameters such as ion ratios and ion excesses, as well as mineral saturation indices, gives useful input into geological, geochemical and geomorphological mapping. These tools will be enhanced for specific regional studies in ongoing research as part of the “Continental Scale Hydrogeochemistry” initiative.

References

- APHA, 1995. Standard methods for the examination of water and wastewater. American Public Health Association: Washington.
- Bardwell, N. and Gray, D.J., 2016a. Hydrogeochemistry of Queensland. Data release: Accompanying Notes. EP156406. 22 p.
- Bardwell, N. and Gray, D.J., 2016b. Hydrogeochemistry of Northern Territory. Data release: Accompanying Notes. EP156405. 21 p.
- Bardwell, N. and Gray, D.J., 2016c. Hydrogeochemistry of Western Australia. Data release: Accompanying Notes. EP156404 CSIRO, Australia. 33 p.
- de Caritat, P., Kirste, D., Carr, G. and McCulloch, M., 2005. Ground water in the Broken Hill region, Australia; recognising interaction with bedrock and mineralization using S, Sr and Pb isotopes. *Applied Geochemistry*: 20, 767-787.
- Drever, J.I., 1982. *The Geochemistry of Natural Waters*. Prentice-Hall, Inc., Englewood Cliffs, N.J. U.S.A. 388 p.
- Forbes, C., van der Hoek, B., Gray, D.J., Hill, S.M., Giles, D. Normington, V., Anand, R.A., Dietman, B.J., Johnson, A.K., McLennan, Reid, N., Rollison, L. Salama, W., Stoate, K. and Wolff, K., 2013. Geological and Hydrological Atlas of the Gawler Craton, South Australia. DET CRC Report Number 2013/326
- Giblin, A.M., 2001. Groundwaters: geochemical pathfinders to concealed ore deposits. A handbook of recommended procedures for sample collection, analyses and some methods of data interpretation for exploration. CSIRO Division of Exploration and Mining, 2001 70 pp.
- Gray, D.J., 2001. Hydrogeochemistry in the Yilgarn Craton. *Geochemistry: Exploration, Environment, Analysis*: 1, 253-264.
- Gray, D.J., 2016a: Hydrogeochemistry Dataset from Stygofauna Sampling, Pilbara Region, Western Australia: Data Release. v1. CSIRO. Data Collection. <http://doi.org/10.4225/08/575CDF639A59A>
- Gray, D.J., 2016b. Integration of Historic Groundwater Data into the Continent Scale Geochemistry Initiative. Submitted to Australian Journal of Earth Sciences.
- Gray, D.J., and Bardwell, N., 2016a. Hydrogeochemistry of South Australia. Data release: Accompanying Notes. EP156406 CSIRO, Australia. 34 p.
- Gray, D.J., and Bardwell, N., 2016b. Hydrogeochemistry of Victoria. Data release: Accompanying Notes. EP158526 CSIRO, Australia. 28 p.
- Gray, D.J., and Bardwell, N., 2016c. Hydrogeochemistry of New South Wales. Data release: Accompanying Notes. EP162242 CSIRO, Australia. 37 p.
- Gray, D.J. and Noble, R.R.P., 2006. Nickel hydrogeochemistry of the northeastern Yilgarn Craton, Western Australia. CRC LEME Open File Report 243R / CSIRO Exploration and Mining Report P2006/524. 133 p.
- Gray, D.J., Reid, N., Dick, S. and Flitcroft, P., 2012. Pilot Hydrogeochemical investigations in the Thomson Orogen, New South Wales. CSIRO Report EP125537, GSNSW Report GS2012/0972, Australia. 29 p.
- Gray D.J., Reid, N., Parker, P and Hughes, K., 2015 Hydrogeochemical Investigations in the Wagga Wagga Region. CSIRO Report EP151283, GSNSW Report GS2015/0219. Australia. 49 p.
- Gray, D.J., Noble R.R.P., Reid, N., Sutton, G.J. and Pirlo, M.C., 2016. Regional Scale Hydrogeochemical Mapping of the Northern Yilgarn Craton, Western Australia: A new Technology for Exploration in Arid Australia. *Geochemistry: Exploration, Environment, Analysis*, 16: 100-115.
- Halse, S.A., Scanlon, M.D., Cocking, J.S., Barron, H.J., Richardson, J.B. and Eberhard, S.M., 2014. Pilbara stygofauna: deep groundwater of an arid landscape contains globally significant radiation of biodiversity. *Records of the Western Australian Museum, Supplement*: 78, 443-483.
- Parkhurst, D.L., Thorstenson, D.C. and Plummer, L.N., 1980. PHREEQE, a computer program for geochemical calculations. U.S. Geological Survey Water Resources Investigations 80 96, 210p.
- Radke, B.M., Ferguson, J., Cresswell, R.G., Ransley, T.R., and Habermehl, M.A., 2000. Hydrochemistry and implied hydrodynamics of the Cadnaowie – Hooray Aquifer, Great Artesian Basin, Australia. Bureau of Rural Sciences, Commonwealth of Australia, Canberra, 229pp.
- Schwab, A.P. and Lindsay, W.L., 1983. Effect of redox on the solubility and availability of iron. *Soil Science Society of America Journal*. 47, 201-5.

CONTACT US

t 1300 363 400
+61 3 9545 2176
e enquiries@csiro.au
w www.csiro.au

FOR FURTHER INFORMATION

CSIRO Mineral Resources
David J Gray
t +61 8 64368678
e david.gray@csiro.au

YOUR CSIRO

Australia is founding its future on science and innovation. Its national science agency, CSIRO, is a powerhouse of ideas, technologies and skills for building prosperity, growth, health and sustainability. It serves governments, industries, business and communities across the nation.